CHALMERS
UNIVERSITY OF TECHNOLOGY

Feasible DC Voltage Levels in Households

Investigation of the efficiency for a DC distribution system in a residential building

Master's thesis in Electric Power Engineering

FREDRIK IDEGÅRD

Department of Electric Power Engineering
CHALMERS UNIVERSITY OF TECHNOLOGY
Gothenburg, Sweden 2022

Master's thesis 2022

Feasible DC voltage levels in households

Investigation of the efficiency for a DC distribution system in a residential building

FREDRIK IDEGÅRD

CHALMERS
UNIVERSITY OF TECHNOLOGY

Department of Eletric Power Engineering
Chalmers University of Technology
Gothenburg, Sweden 2022

Feasible DC Voltage Levels in Households
Investigation of the efficiency for a DC distribution system in a residential building
FREDRIK IDEGÅRD

Supervisor: Patrik Ollas, PhD student at RISE
Examiner: Torbjörn Thiringer, Professor, Electrical Engineering Department

Master's Thesis 2022
Department of Electrical Power Engineering
Chalmers University of Technology
SE-412 96 Gothenburg
Telephone +46 31 772 1000

Gothenburg, Sweden 2022

Feasible DC voltage levels in households
Investigation of the efficiency for a DC distribution system in a residential building
FREDRIK IDEGÅRD
Department of Electrical Power Engineering
Chalmers University of Technology

Abstract

Alternative current (AC) power distribution has been considered superior to direct current (DC) power distribution since the late 1800s. Development in the power electronics field has made DC power systems more efficient and competitive. Almost all electrical loads in a residential building operate on DC at their final stage, which is another motivation for DC power distribution.

This thesis investigates the energy-saving potential of implementing a DC grid in a residential building compared to a conventional AC topology grid. A synthetic load profile of the annual electric energy consumption was created and tested. The load profile was tested with several different setups where different supply voltage levels and converter efficiencies were compared.

Of the modelled cases, the 380 VDC system performed best with constant efficiencies for converters and rectifiers with a system efficiency of 97.8%, just 0.01% better than the AC system. For load-dependent efficiency, the 230 VAC performed the best with an efficiency of 96.1%, whereas the 380/48 VDC system had the worst performance with an efficiency of 90.6%.

Acknowledgements

I want to express my deepest gratitude to everyone who has supported me and believed in me during this thesis work.

Firstly I want to thank my lovely girlfriend Annie and daughter Signe. Also, my parents and sister who been a great support throughout the work.

Then I want to thank my supervisor Patrik Ollas and examiner Torbjörn Thiringer who have been supportive and patient. I also want to thank RISE for allowing me to work on this thesis.

Finally, I would like to thank my friends who supported me, especially Erik Ivarsson, Rasmus Hagman, and Rasmus Karlsson who have always been by my side at Chalmers.

FREDRIK IDEGÅRD Gothenburg, 2022

Contents

1

Introduction

1.1 Background

The planet is facing a major environmental challenge and must become sustainable. Every sector in society must become more energy efficient to make this possible. The residential sector constitutes 26.9% of the world's electrical usage [1]. Since the late 1800s, when Thomas Edison was defeated in "the war of currents" by Nikola Tesla, AC has typically been considered the superior choice in electric power distribution [2]. A deciding factor in the preference for AC over DC is the ease of transformation to different voltage levels, resulting in cheaper energy transport. Due to development in the power electronics field, DC distribution is again a possible candidate for electric power distribution [3]. DC sources, such as photovoltaic (PV) cells and batteries for storage have also seen significant development since the days of Tesla and Edison. There is also an increased amount of native DC-operated loads, e.g. electric cars, that could benefit from DC distribution.

1.2 Literature Review

Many works and research already exist concerning the subject of AC vs DC distribution. In different works, the results of energy savings potentials vary in the range of 1.9–25% when AC is replaced by DC [4, 5, 6, 7]. This variation in results is explained by the specific assumptions and losses that have been considered. In [8], several studies regarding DC grids are evaluated regarding how the authors handled load modelling, power electronics efficiency, storage, voltage level, line losses, and distributed energy. A common assumption is to use constant efficiencies for power electronic converters (PECs), which often underestimate the losses [6]. These six mentioned factors affect the total efficiency of a system and explain why the result differs and makes it hard to deliver a verdict on whether AC or DC systems are superior. Of these six factors, load modelling and converter efficiencies were considered to have the greatest impact on energy consumption and line losses could play a decisive part [8]. Conduction losses are not considered in many works [5, 9, 10], and in some works, they were included, but the feeder lengths were chosen arbitrarily [11].

1.3 Purpose

This thesis investigates the possible energy savings in a residential building's electric power distribution powered by DC compared with AC. Within this, a goal is to quantify saving opportunities through the life cycle cost (LCC).

2
Theory

2.1 Electrical Losses in Buildings

For the distribution system there are two types of losses considered in this study: losses in PECs and cable conduction losses.

2.1.1 Losses in Power Electronic Converters

In this thesis PECs are used in the forms of rectifiers and DC-DC converters. Rectification losses occur when the system rectifies AC to DC and a DC-DC converter is used for stepping up or down between different DC voltage levels. The efficiency for power electronic converters is calculated by

$$\eta(t) = \frac{p_{out}(t)}{p_{in}(t)} \tag{2.1}$$

where $p_{in}(t)$ is input power, $p_{out}(t)$ is output power, $\eta(t)$ is the efficiency. Losses for power electronic converters can be expressed as

$$p_{loss}(t) = p_{in}(t) - p_{out}(t) \tag{2.2}$$

Rewriting (2.1) and inserting into (2.2) gives

$$p_{loss}(t) = p_{out}(t)\left(\frac{1}{\eta(t)} - 1\right). \tag{2.3}$$

2.1.2 Conduction Losses

Conduction losses in cables occur during power transmission and is calculated as

$$p_c(t) = Ri^2(p) \tag{2.4}$$

where $p_c(t)$ is the conduction loss, R is the resistance of the cable and $i(t)$ the current through the cable. Cable resistance, R, is calculated as

$$R = 2\rho\frac{L}{A} \tag{2.5}$$

where ρ is the resistivity for the cable material, L is the length of the cable, and A the cross-sectional area of the cable. The reason for the ”2” is to include conduction

losses on the way back from an appliance. The cross-sectional area is selected by looking into thermal conditions according to the IEC 60228 standard [12]. There is also an inductive part for the AC case but this has been neglected since it will not significantly impact the result. The cable current is calculated as

$$i(p) = \frac{p_{load}(t)}{v(t)} \tag{2.6}$$

where $p_{load}(t)$ and $i(p)$ is the power and current, respectively, of an appliance at time t and $v(t)$ is the voltage over the same appliance.

2.2 Power Electronic Converters

Power electronic converters are used for control and conversion of electric power. Power electronics are made of different semi conductor devices like diodes, thyristors and power transistors.

2.2.1 Rectifier

To transform electrical signals from AC to DC a rectifier is needed. In Fig. 2.1, the design of a single-phase full-wave bridge rectifier is shown. The polarity of the incoming voltage source controls which path the current takes. During the positive half of the duty cycle for V_{in}, the current takes the green path through the diodes D_1 and D_4 while D_2 and D_3 are reversed biased. During the second half of the duty cycle the current instead goes along the red path through D_2 and D_3 while D_1 and D_4 are reverse biased [13]. In Fig. 2.2, curves for one period for input and output voltage can be seen.

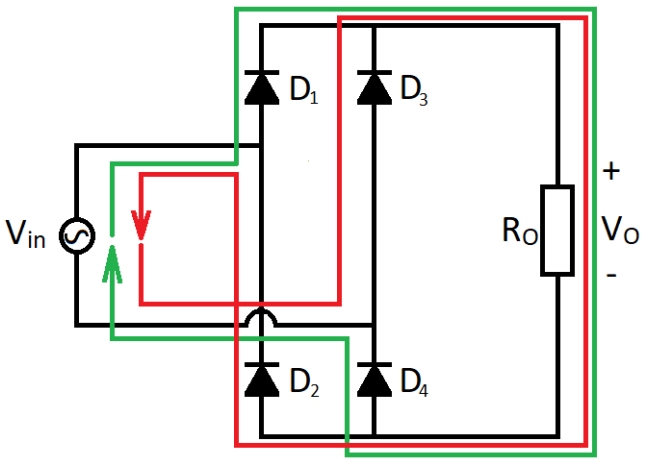

Figure 2.1: A single phase full-wave bridge rectifier. The current path during the positive input voltage is shown by the green line and the current path during the negative input voltage period is shown by the red line.

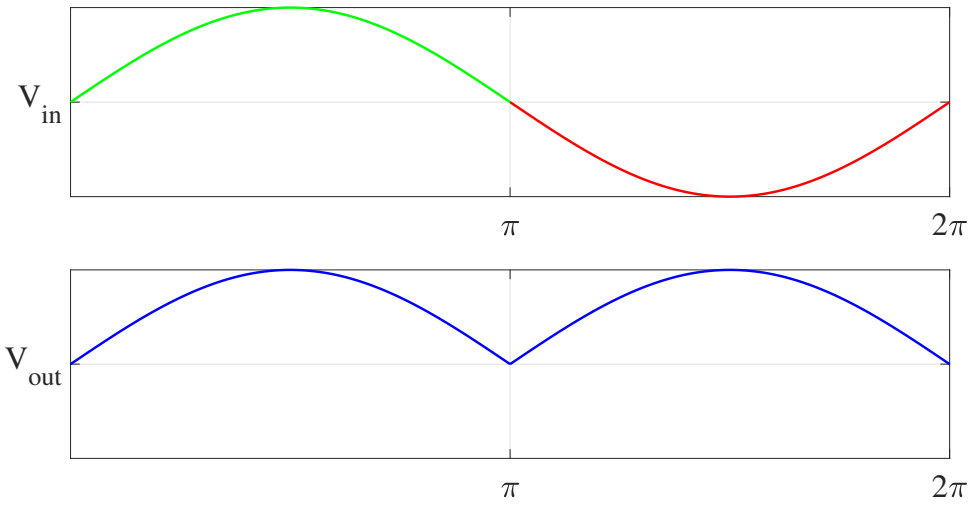

Figure 2.2: The input voltage is represented with a green line for the first half of the period and a red line for the second half of the period. The output voltage is represented with a a blue line for the whole period.

2.2.2 DC-DC Converter

A DC-DC converter is used to step-up (boost) or step-down (buck) between DC voltage levels. Several types of DC-DC converters are available; in Fig. 2.3, a dual active bridge (DAB) DC-DC converter is shown and used in this study. To explain the working principle, Q_{11}-Q_{24} can be seen as switches that turn ON/OFF to create a path for the current from the input to the output. By using advanced controls, which are further explained in [14], high efficiency can be obtained over a wide converter load range.

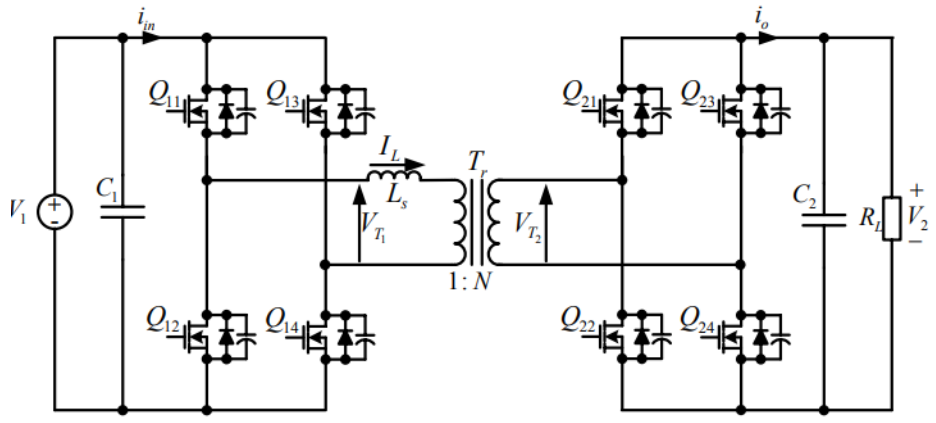

Figure 2.3: Topology of a dual active bridge DC-DC converter retrieved from [14].

2.3 Electrical System Topologies in Residential Buildings

Three different topologies are presented in this report. The first one is an AC topology, the other two are variations of DC systems. The difference between the DC variants is that one has one voltage level and the other has two voltage levels.

2.3.1 AC Topology

The most common power distribution system for a residential electrical system today is by far AC. Figure 2.4 shows a typical topology for a residential AC system. All loads are expected to operate on DC at their final stage.

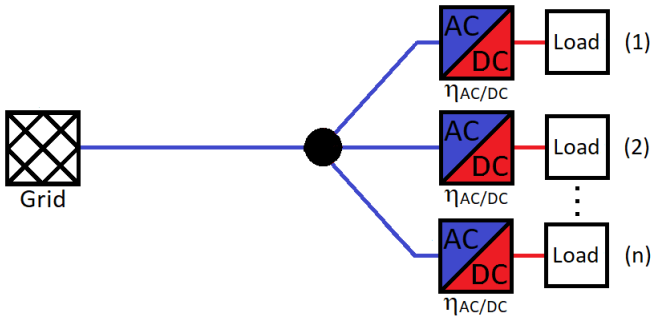

Figure 2.4: AC electrical system for a residential building. Blue color represents AC parts and red color DC parts of the system.

In Fig. 2.4, "n" is the number of appliances in the AC system and each appliance has its individual rectifier. To calculate how much power is drawn from the grid all loads and losses that occur at the same time are summed up according to

$$p_{grid}(t) = \sum^{n} \left[p_{load,n}(t) + p_{cond.,n}(t) + p^{rect}_{loss,n}(t) \right] \tag{2.7}$$

where $p_{grid}(t)$ is the power drawn from the grid, $p_{load,n}(t)$ is the power drawn by active loads at time t, $p_{cond,n}(t)$ are conducting losses at time t, $p^{rect}_{loss,n}(t)$ are rectification losses at time t, and n is the number of fuses. Rectification losses are calculated according to

$$p^{rect}_{loss,n}(t) = \sum^{k} \left[\frac{p_{load,k}(t)}{n_{rec}(t)} - p_{load,k}(t) \right] \tag{2.8}$$

where $p^{rect}_{loss,n}(t)$ is the rectification loss for a fuse at time t, $p_{load,k}(t)$ the power drawn from a load, $n_{rec}(t)$ the efficiency for the load and k the number of loads connected to fuse n.

2.3.2 DC Topology Without Sub-level

Figure 2.5 shows a DC system with one voltage level that has a single rectifier to all loads instead of individual ones as in the AC system shown in Fig. 2.4. Power taken

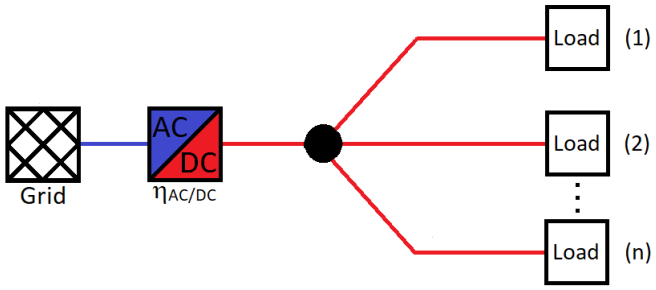

Figure 2.5: Electrical system for a residential building supplied with DC. Here a single central grid connected rectifier is used instead of several individuals to each appliance.

from the grid is calculated as in (2.7) with the difference that $p^{rect}_{loss,n}(t)$ is calculated according to

$$p^{rect}_{loss,n}(t) = \Big(\frac{1}{\eta_{rec}(t)} - 1\Big) \sum^{n} \Big[p_{load,n}(t) + p_{cond,n}(t)\Big] \tag{2.9}$$

where $p^{rect}_{loss,n}(t)$ is the rectification loss for a fuse at time t, $p_{load,n}(t)$ the power drawn from a load, $p_{load,n}(t)$ is the conduction loss, $n_{rec}(t)$ the efficiency for the grid rectifier and n is the number of loads connected to rectifier.

2.3.3 DC Topology With a Sub voltage level

In Fig. 2.6, a sub voltage level DC network has been added through a DAB DC-DC converter. Loads are divided between the two parallel networks based on their rated power. For the low voltage DC (LVDC) network, a maximum power limit is set, loads with rated power below the maximum power limit is connected to the LVDC and loads with rated power higher than the power limit is connected to the network with higher voltage. Power taken from the grid for this setup is calculated in a similar way as the DC topology without sub voltage level with the difference that a converter loss, $p^{conv}_{loss,n}(t)$, is added according to

$$p_{grid}(t) = \sum^{n} \Big[p_{load,n}(t) + p_{cond.,n}(t) + p^{rect}_{loss,n}(t) + p^{conv}_{loss,n}(t)\Big] \tag{2.10}$$

where $p^{rect}_{loss,n}(t)$ is the rectification loss for a fuse at time t, $p_{load,k}(t)$ the power drawn from a load, $n_{rec}(t)$ the efficiency for the load and k the number of loads connected to fuse n. The rectifer losses are calculated according to

$$p^{rect}_{loss,n}(t) = \Big(\frac{1}{\eta_{rec}(t)} - 1\Big)\Big(p^{conv}_{loss}(t) \sum^{k} \Big[p_{load,k}(t) + p_{cond,k}(t)\Big]\Big) \tag{2.11}$$

where $p^{rect}_{loss,n}(t)$ is the rectification loss for all fuses at time t connected to the rectifier, $p_{load,n}(t)$ the power drawn from a load, $p_{cond,n}(t)$ is the conduction loss, $n_{rec}(t)$ the efficiency for the grid rectifier and n is the number of loads connected to rectifier. The converter loss in (2.10) is calculated according to

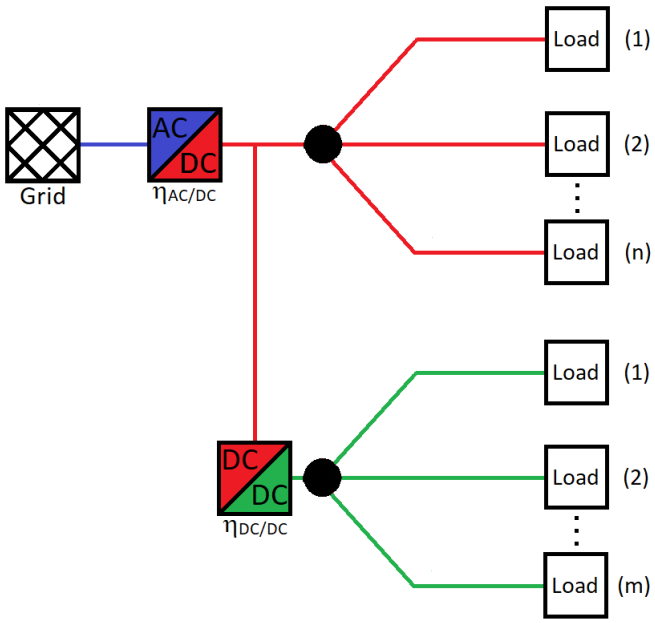

Figure 2.6: DC Electrical system for a residential building with two DC voltage networks. A parallel LVDC network is created by a DAB DC-DC converter for smaller loads.

$$p_{loss}^{conv}(t) = \Big(\frac{1}{\eta_{conv}(t)} - 1\Big) \sum^{m} \Big[p_{load,m}(t) + p_{cond,m}(t)\Big] \tag{2.12}$$

where $p_{loss}^{conv}(t)$ is the converter loss for all fuses at time t connected to the converter, $p_{load,m}(t)$ the power drawn from a load, $p_{cond,m}(t)$ the conduction loss, $n_{conv}(t)$ the efficiency for the converter and m is the number of loads connected to converter.

3

Case Setup

3.1 The Research Villa

The cases investigated in this work are based on layouts and measurements from a testbed facility called the research villa [15]. The research villa is a net-zero energy building constructed to investigate energy usage in a residential building. The residential building is equipped with a geothermal ground-source heat pump that provides space heating and domestic hot water. The research villa is certified according to Miljöbyggnad level gold and it is equipped with measurement devices to monitor the villa's performance. The research villa is a two-story villa, Fig. 3.1 and 3.2 show the layout [16]. In Fig. 3.1, a green circle marks where the incoming AC power is connected. Each room has been assigned a number that is used to explain in which rooms various devices have been placed.

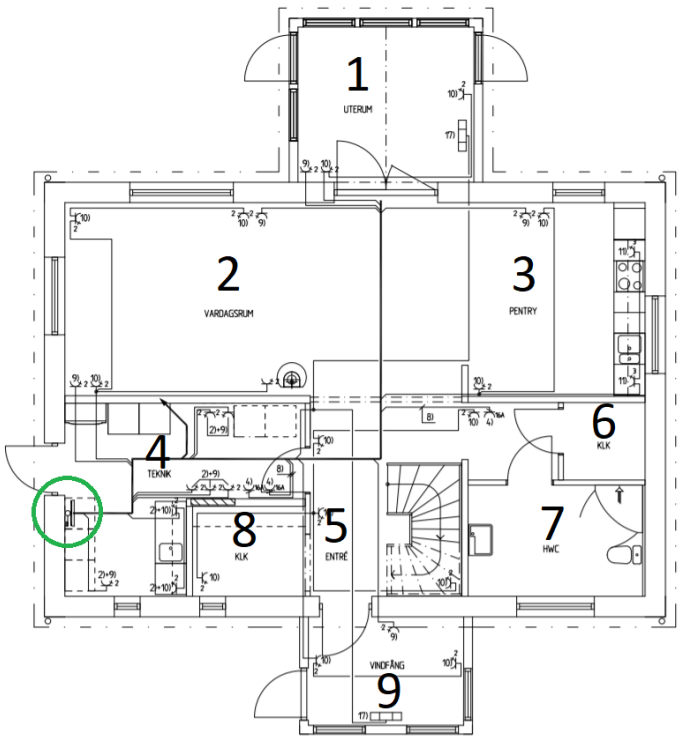

Figure 3.1: Layout of the first floor of the research villa. The green circle marks where the incoming grid power is connected.

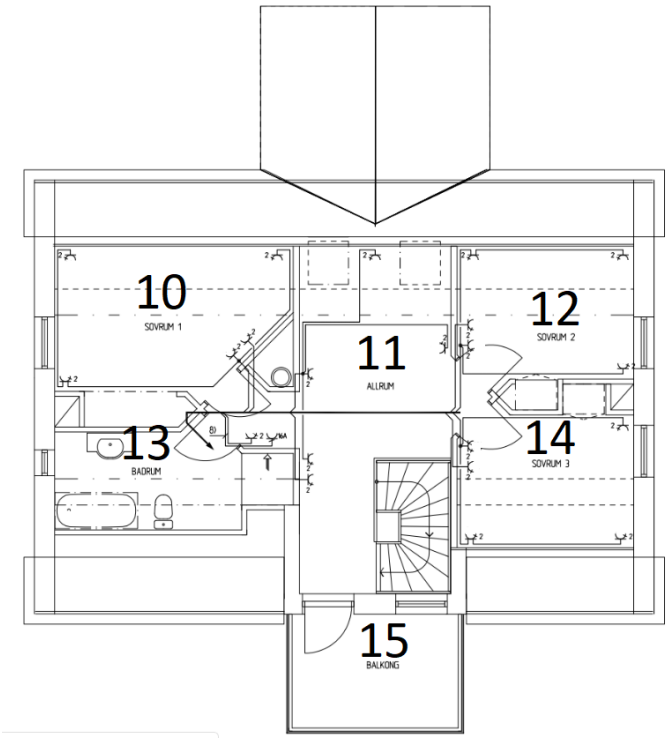

Figure 3.2: Layout of the second floor of the research villa. The green circle marks where the wires are coming up from the first floor.

The measured data is recorded with a 15-minute temporal resolution. Figure 3.3 shows accumulated daily energy use during 2016 for the research villa for the four load types heat pump, ventilation, miscellaneous appliances and lighting. In Fig. 3.3, a seasonal behavior is observed for the aggregated energy, where the research villa uses more energy during winter than in summer. The seasonal variation is explained by the weather, the winter season is colder and darker than the summer season in Sweden. Because of this difference between winter and summer, the heat pump operates harder during winter to maintain the space heating demand. The recorded data from the villa is divided into four subcategories: space heating and domestic hot water generation (from the heat pump), ventilation, lighting, and miscellaneous appliances. Ventilation is handled by a device called FTX that controls the exhaust air and supplies air to recycle heat in the building. Lighting includes all the ceiling lights, and miscellaneous appliances include the rest of the household appliances, e.g. washing machine, dishwasher, etc. Table 3.1 shows the recorded values for the research villa's annual energy consumption during 2016 for each of these four posts.

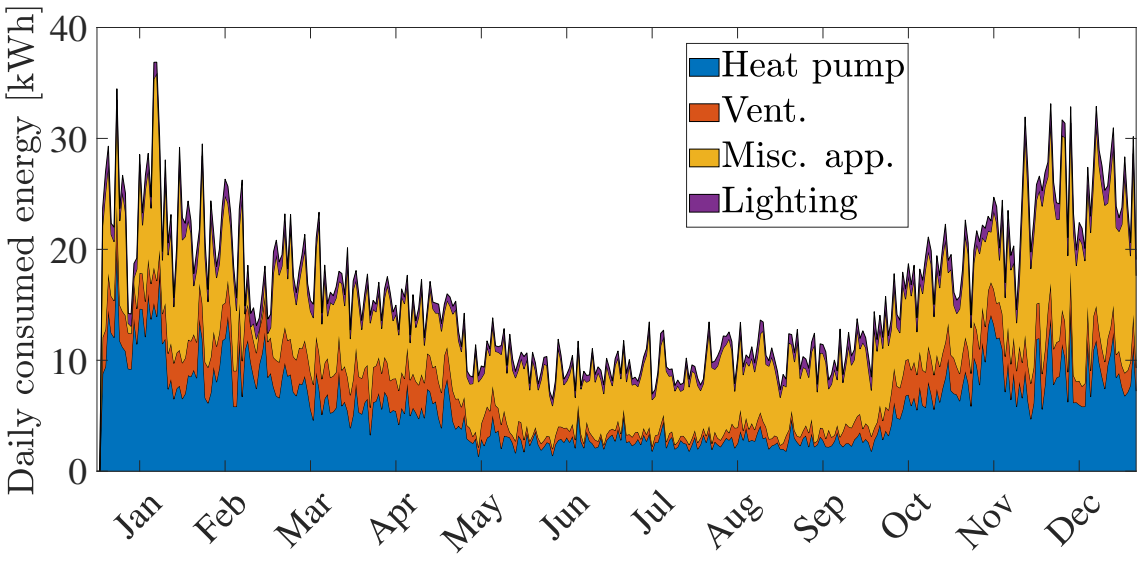

Figure 3.3: Consumed electrical energy in 2016 for the research villa. Each point is the sum of all consumed energy over a day.

Table 3.1: Measured consumed electric energy for the different categories over one year.

Load Channel	Consumed Energy [kWh]
Space heating	2205
Ventilation	801
Lighting	359
Misc. appliances	2580
Total	5945

3.2 Synthetic Load Profiles

Of the recorded load profiles, space heating and ventilation are used directly from the recorded measurements, while the other two are replaced with synthetic profiles. The reason for this is that the sets of data only tell the aggregated energy over the last 15 minutes without specifying which appliance is used. The appliance time-identification is needed to apply the right cable length L in (2.5) to recieve the correct conduction loss. To create the synthetic load profiles the following criteria (Cn) were used:

C1 The total amount of aggregated energy for the synthetic load profiles should be within $\pm 5\%$ of the recorded data from the research villa over a period of one year.

C2 The duration curves are compared to check that the recorded and synthetic load profiles have similar power peaks.

C3 Appliances should be active at reasonable times e.g. no cooking in the middle of the night.

C4 Interplay between different appliances e.g. the stove and kitchen fan is active at the same time.

To fulfill the goal of having the same aggregated energy and get a seasonal variation for the energy usage, the recorded data are divided into four sets. A set represents one season e.g., the measured aggregated energy during March–May represents spring. By deciding which months should represent each season it is just to take the aggregated energy during these months and divide it by the number of weeks during the same period. This results in a target value for how much aggregated energy each seasonal week should contain. This target value is calculated as

$$SW_{mean} = \frac{\sum E_{season}}{n_{weeks}} \tag{3.1}$$

where SW_{mean} is the average consumed energy for a seasonal week, E_{season} is the aggregated energy during the whole season and n_{weeks} is the number of weeks during that season. The target values for the load profiles are displayed in Table 3.2.

Table 3.2: Aggregated Energy for a week during different seasons.

Seasonal week	Lighting [kWh]	Misc. appliances [kWh]
Winter week	9.3	64.1
Spring week	5.7	42.4
Summer week	4.6	39.3
Fall week	7.2	45.7

3.2.1 Synthetic Load Profile Verification

All loads considered in this study are listed in Tables 3.3–3.4 with their rated power values, and for miscellaneous appliances in Table 3.4 the annual energy consumption is also included. In Tables 3.3–3.4 location and quantities are indicated by addressing in which room an appliance is placed. Smaller devices that are often moved around and used at several locations, e.g. a cell phone, have been assigned a fixed location to simplify the calculations.

Table 3.3: Ceiling lights in the research villa and their position in Fig. 3.1-3.2 and rated power.

Loads	Abbreviation	Rated power [W]	Room & quantity														
			1	2	3	4	5	6	7	8	9	10	11	12	13	14	15
Case wall	L1	6															10
Case LED	L2	4											2				
Bright eye tilt	L3	6.7	6	11	6		7			2	6	3	7	3	5	3	
Bright eye IP44	L4	6.7							6								
Led dot	L5	1.2		2	1							1		1		1	
Moon	L6	10		2	1	3		1					1				
Sink LED	L7	24			1	1			1						1		
Lamp post	L8	9															2

Table 3.1 showed that during a year miscellaneous appliances consume 2580 kWh, to meet the compliance of $C1$, household appliances and their operation is

developed. When household appliances were selected, the focus was on finding appliances with good energy performance by today's standard, but it was not a focus to find the most efficient one for each appliance. For larger devices e.g., a washing machine often the annual energy, cycles per year, and rated power are shown while for smaller devices like a coffee machine only rated power is shown. Therefore, the load profiles for appliances where no annual energy consumption was shown have been made by assumptions considering when people are home and typically use the appliance. For example, coffee is often made for breakfast, therefore the coffee machine should be active during the morning hours. The abbreviations in Tables 3.3–3.4 are used in Fig. A.1–A.6 in the appendix and all appliances are available to find at [17].

Table 3.4: Miscellaneous appliances with their rated power and annual energy consumption for synthetic load profiles [17].

Loads	**Abbreviation**	**Annual energy [kWh]**	**Rated power [W]**	**Room**
Stovetop/oven	SO	377	9000	3
Dish washer	DW	259	2000	3
Microwave oven	MW	61	600	3
Washing machine	WM	249	500	4
Dryer	D	242	3000	4
Coffee machine	CM	125	1000	3
Heat pump	HP	2200	6000	4
Ventilation	FTX	800	1250	4
Vacuum cleaner	VM	144	1000	5
Water kettle	WK	84	1200	3
Hair dryer	HD	78	1000	13
Kitchen fan	KF	29	200	3
Fridge/freezer	FF	397	195	3
TV1	TV	88	100	2
TV2	TV	111	100	11
Gaming console	GC	168	137	11
Modem	M	33	6	2
Router	R	33	6	2
Laptop	C	19	21	2
Cell phone 1	CP1	4	6	10
Cell phone 2	CP2	4	6	10
Cell phone 3	CP3	4	6	12
Cell phone 4	CP4	4	6	14

In Fig. 3.4, criteria $C2$ from Section 3.2 is checked by comparing the duration curves between the recorded and synthetic load profiles. This is done to ensure that the synthetic load profile behaves similarly to the recorded ones and avoid unrealistic power peaks.

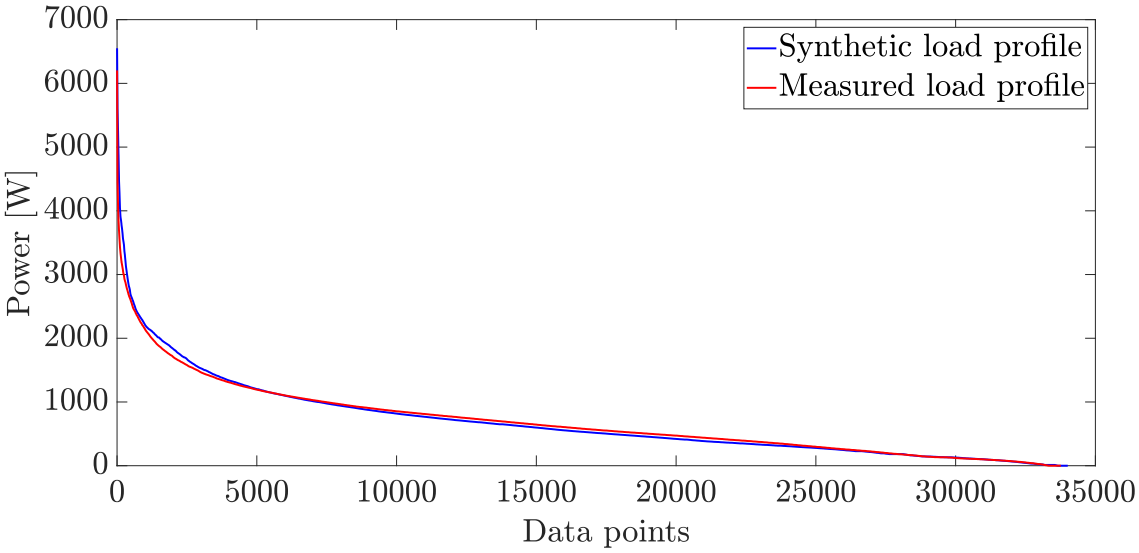

Figure 3.4: Duration curves for all loads in the research villa. The red line represent the measurement data and the blue line is the synthetic profile.

The root mean square error (RMSE) [18] for the two curves in Fig. 3.4 is calculated according to

$$RMSE = \sqrt{\sum_{i=1}^{n} \frac{(SP_i - RP_i)^2}{n}} \tag{3.2}$$

where SP_i is the synthetic load profile, RP_i is the recorded load profile and n is the number of measurements. The RMSE for load profiles in Fig. 3.4 is 77.6 W. To evaluate the result of the RMSE, the result is normalized according to

$$NRMSE = \frac{RMSE}{max - min} \tag{3.3}$$

where $NRMSE$ is the normalized root mean square error, $RMSE$ the root mean square error from (3.2), max the maximum value of the load profile and min the minimum value of the load profile. The result is a number between 1 and 0, with zero indicating a perfect match. NRMSE for the curves in Fig. 3.4 is 0.013, which is a satisfying result.

3.2.2 Load Profiles for Loads with Large Power Variation

Each load receives an individual set of data points that represent its load profile. Most loads have an ”ON/OFF” operation where the ON value is equal to its rated power. Exceptions have been made for dishwasher, dryer, and washing machine. These appliances are assumed to perform a sequence of data points when they are

turned on which represents a program for an appliance. The main focus in these profiles has been the aggregated energy and reaching the rated power of the machine at least once during a program. The profiles for these programs are created with inspiration from [19, 20]. Figure 3.5 shows the load profile for a dishwasher program and how the dishwasher requires the most power for heating up water. Water is heated twice during a program and during one of these times it reaches its rated power of 2 kW. Load profiles for other appliances with large power variation are shown in Fig. A.7–A.8.

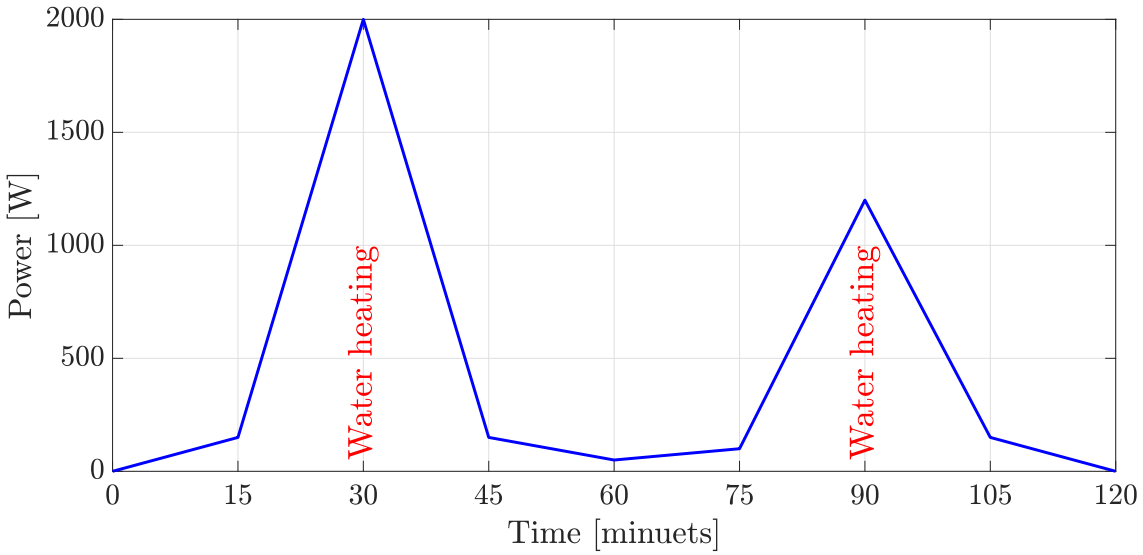

Figure 3.5: Load profile for a program of a dishwasher. Most of the energy is needed to heat up water.

3.3 Line Loss Calculations

The importance of using the right number of active loads to receive the right amount of power and cable length in (2.4) respectively (2.6) can be explained with an example. In this example a couple of assumptions have been made to simplify calculations: lengths between each load are equal and every load has the same rated power. Then a scenario for a fuse with n number of loads can be presented as in Fig. 3.6.

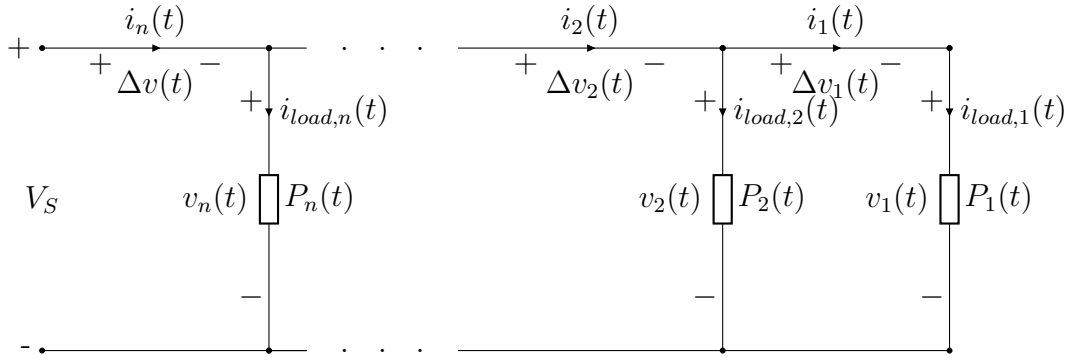

Figure 3.6: Layout of a circuit representing a fuse with n loads.

In Fig. 3.6, $i_1(t)$-$i_n(t)$ are the currents between loads, $i_{load,1}(t)$-$i_{load,n}(t)$ are the currents through the loads, V_S the voltage source for the fuse, $\Delta V_1(t)$-$\Delta V_n(t)$ voltages over each load and P_1-P_n the powers for each load. From Fig. 3.6 the conduction loss can then be expressed as

$$\begin{aligned} p_{c,n}(t) &= p_{c,n}(t) + ... + p_{c,2}(t) + p_{c,1}(t) \\ &= Ri_n^2(t) + ... + Ri_2^2(t) + Ri_1^2(t) \end{aligned} \tag{3.4}$$

If it is further assumed that the voltage drop between loads is negligible, the current can be expressed in terms of i_1 as

$$\begin{aligned} &i_1(t) \approx i_{load1}(t) \\ &i_2(t) \approx i_{load1}(t) + i_{load2}(t) && \Rightarrow i_2(t) \approx 2i_1(t) \\ &i_n(t) \approx i_{load1}(t) + i_{load2}(t) + ... + i_{loadn}(t) && \Rightarrow i_n(t) \approx ni_1(t) \end{aligned}$$

Now 3.4 can be rewritten as

$$\begin{aligned} p_{c,n}(t) &= R(ni_1(t))^2 + ... + R(2i_1(t))^2 + R(i_1(t))^2 \\ &= n^2Ri_1^2(t) + ... + 4Ri_1^2(t) + Ri_1^2(t) \\ &= n^2p_{c,1}(t) + ... + 4p_{c,1}(t) + p_{c,1}(t) \end{aligned} \tag{3.5}$$

3.4 Dynamic and Constant Efficiency for Power Electronics

Typically, a constant efficiency is used in previous works. To better represent reality, a load-dependent efficiency can be used, so called dynamic efficiency. In a related work [8], both dynamic and constant efficiency was used to quantify the difference between the two approaches. A constant efficiency is often used to simplify investigations while a dynamic load-dependent efficiency more realistically models the characteristics of both rectifiers and converters. In this study the constant efficiency for the AC to DC rectification is set to 97.8% [21], and for the dynamic efficiency a load-dependent reference curve is retrieved from [22]. Load dependency is calculated according to

$$\eta(p) = \frac{p(t)}{P_{max}} \tag{3.6}$$

where $\eta(p)$ is the efficiency, $p(t)$ the power at time t and P_{max} the rated power of the PEC. The results from (3.6) are then interpolated with the reference curve from [22] to retrieve load dependent efficiency curves for power electronics. In Fig. 3.7, the reference curve from [22] is plotted together with the constant efficiency at 97.8%.

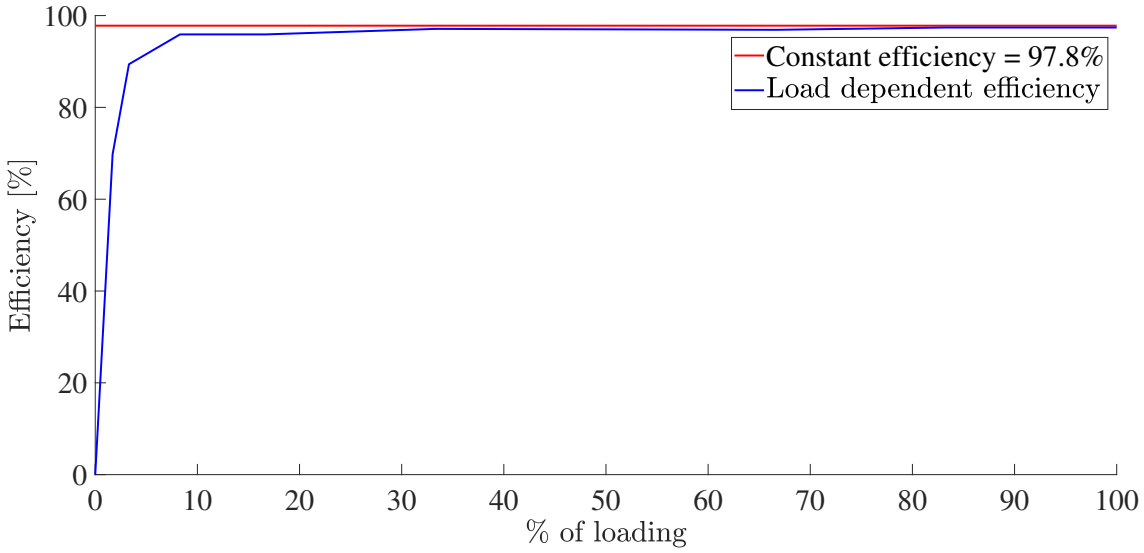

Figure 3.7: Constant efficiency is represented by the red line and the blue line represents the load dependent efficiency curve. The reference curve for the load dependent efficiency comes from [22].

Figure 3.7 shows that the load dependent efficiency lies below the constant efficiency at all times, especially when working at levels below 10% of the maximum loading.

3.5 Case Studies

Four cases are modeled for this study 230 VAC, 380 VDC, 380/48 VDC, and 380/20 VDC. 230 VAC is the conventional electrical system for households today, and for DC systems 380 VDC is the leading choice among scientists [23]. To increase personnel safety, extra low voltage levels (SELV) are introduced. A parallel 48 VDC is grid tested in one case and a 20 VDC grid is introduced in another. The 20 VDC is an interesting voltage level due to its capability within USB-C [24]. Each case is run four times in total. The first two times with constant rectifier and converter efficiency, then two times with dynamic efficiencies for rectifiers and converters. All cases run two times to receive information for the life cycle cost analysis, in the first run all cable areas are based on thermal condition and set to their minimum allowed area. The second run investigates if it could be more economic over time to use a larger cable area. The first and second run is to be referred to as standard and optimized, respectively, in Table 3.5.

Table 3.5: All cases that will be run in this study.

	A_{cable}	**Constant** η	**Dynamic** η
Case_i	Standard	x	x
	Optimized	x	x

The overall efficiency for each case is calculated according to

$$\eta_{case_i} = \frac{\sum P_{load,annual}}{\sum P_{grid,annual}} \tag{3.7}$$

where η_{case_i} is the efficiency, $P_{load,annual}$ the annual power consumed by all loads and $P_{grid,annual}$ the total annual power drawn by the residential building. $P_{load,annual}$ is the same for all cases and found in Table 3.1 and $P_{grid,annual}$ is calculated by (2.7) or (2.10) depending on which case it is.

3.5.1 Reference case 230 VAC

The 230 VAC case is the reference case and represents electric power distribution in a conventional residential building. All conduction losses occur at 230 VAC and every appliance has an individual rectifier. The total power drawn from the grid is calculated according to (2.7), rectification losses according to (2.8) and conduction losses according to (2.4). The dynamic efficiency for individual rectifiers are calculated according to (3.6), where P_{max} is set to the rated power value of the appliance it is connected to. In Fig. 3.8, the 230 VAC case is visualized from the electrical main grid to the loads in the villa. Positions of the fuse box, line losses, rectification losses and loads in the system are marked out.

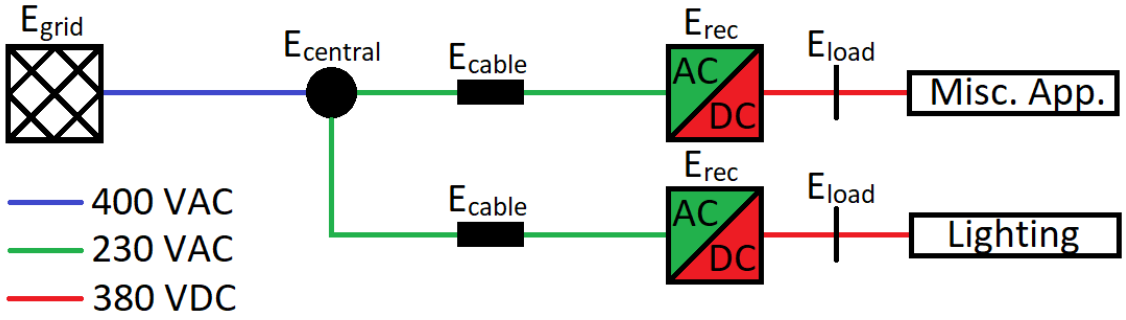

Figure 3.8: The 230 case with line losses, rectification losses and loads positions marked.

3.5.2 Case 2 – 380 VDC

In this case, 230 VAC is replaced with 380 VDC. All conduction losses occurs at 380 VDC, and the individual rectifiers are removed and replaced with a central grid-tied rectifier shown in Fig. 3.9. The total power drawn from the grid is calculated according to (2.7), rectification losses according to (2.9) and conduction losses according to (2.4). The dynamic efficiency for the grid-tied rectifier is calculated

according to (3.6) where P_{max} is set to 13.8 kW. The maximum power output for a 3-phase system with a 20 A fuse, which is commonly used in a conventional AC system for a residential building is 13.8 kW, and therefore the chosen P_{max}.

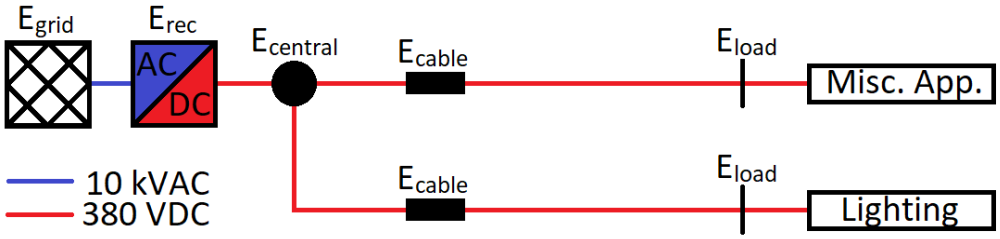

Figure 3.9: An overview of the 380 VDC case where losses and loads are marked.

3.5.3 Case 3 – 380/48 VDC

In this case, a parallel 48 VDC network is added, this network is created by adding a central DC/DC converter. Conduction losses occur on both 380 and 48 VDC levels. Power limit for loads connected to the 48 VDC network is set to 480 W which is based on the assumption that 10 A fuses are used. All appliances connected to the same fuse have a maximum combined power peak below 480 W and are now driven on 48 VDC instead of 380 VDC. The total power drawn from the grid is calculated according to (2.10), rectification losses are calculated according to (2.8) conversion losses are calculated according to (2.12) and conduction loss according to (2.4). For the DC-DC converter, P_{max} is set to the maximum measured power output of all the loads connected to the low voltage DC-grid. In Fig. 3.10 is the layout of the 380/48 VDC system is shown. The DC/DC converter in Fig. 3.10 creates a parallel 48 VDC network.

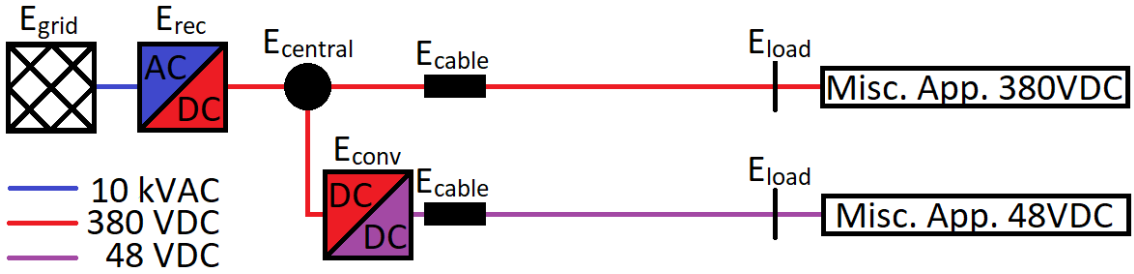

Figure 3.10: Layout of the system used in the 380/48 VDC case. The system has a grid-tied rectifier and a DC/DC converter that bucks the voltage from 380 to 48 VDC.

3.5.4 Case 4 – 380/20 VDC

This case is similar to case 3 but here the parallel network is a 20 VDC network instead of 48 VDC, thus conduction losses are on the 380 and 20 VDC level. 20 VDC is the voltage at which USB-C operates and the power limitation is lowered from 480 W to 100 W which narrows the number of loads for this sub-level [24]. In this

case the power limit is decided by the current limit for USB-C outlets which is 5 A, and not the fuse size. In Fig. 3.11, an overview of the layout for the 380/20 VDC case is shown.

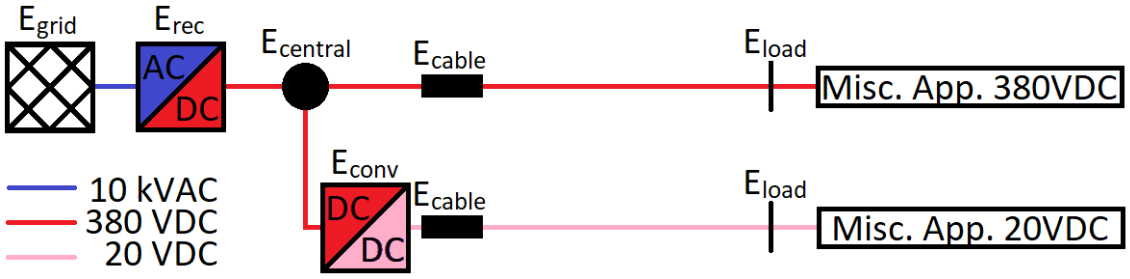

Figure 3.11: Layout of the system used in the 380/20 VDC case. The system has a grid-tied rectifier and a DC/DC converter that bucks the voltage from 380 to 20 VDC.

3.6 Life Cycle Cost

To receive better performance for the system, cable areas can be scaled up to reduce resistance and conduction losses according to (2.4)–(2.5). If the cross-sectional area was to be scaled up conduction losses would drop; but at what cost? To choose the most economical option of cross-sectional area for cables over time, a life cycle cost analysis is made. The initial areas of each cable in (2.5) is determined by the maximum current flowing through the cable [25] and chosen from Table 3.6.

Table 3.6: Cross sections, current limit, resistance per meter and price per meter for cables [25].

Cross section [mm^2]	Current limit [A]	Resistance [Ω]	Price [SEK/m]
0.75	6	22.9	2.01
1.5	10	11.4	3.01
2.5	16	6.88	4.76
4	20	4.30	8.83
6	25	2.86	12.87
10	34	1.72	19.77
16	45	1.08	29.27

Calculations for the LCC is made with the net present value (NPV) equation [26] according to

$$\text{NPV} = -I_0 - \sum_{i=1}^{n} \frac{E_{Loss}(i)E_{Price}(i)}{(1+r)^i} \tag{3.8}$$

where I_0 is the initial cost for cables, E_{Loss} the annual energy loss, E_{Price} the price of electricity, i number of years examined, and r the discount rate. The discount rate is used to calculate the required rate of return over time. E_{Price} is the price for

the bought electricity, with taxes, net fee, etc. included. For this study the price of electricity is fixed at 2 SEK/kWh [1] [27].

$$I_0 = 3\sum_{j=1}^{n} L_{Cable}(j)C_{Price}(j) \tag{3.9}$$

where L_{Cable} is the length of a cable, C_{Price} the price of a cable depending on the area of the cable, j the fuse number examined, and n the total number of fuses in the house. To every appliance there are three wires, two conductors and an earth, hence the 3 in (3.9).

[1] In reality the price for electricity fluctuates during the year and is affected by supplier, type of agreement, where you live etc. Due to the difficulty in accounting for all the factors that influence electricity prices a constant price is assumed. The initial investment, I_0, is calculated as

4

Results

Each case has run four times and to distinguish between the results they have been denoted with subscripts. Subscripts C and D refer to constant and dynamic efficiencies for power electronics respectively. Subscripts 1 and 2 refer to standard and optimized cases, respectively, where the difference is that cable area is adjusted to reduce conduction losses over time. For instance is $230VAC_{D1}$ the reference case with dynamic rectifiers (D) and standard sizes on cables(1).

4.1 Reference Case – 230VAC

Figure 4.1 shows how energy losses are distributed between all fuses for the reference case with a constant PECs efficiency. Two losses occur in the 230 VAC case, rectification and conduction losses. The main loss in this case is rectification loss, and of the fuses the heat pump is by far the greatest energy consumer which also leads to most losses. The heat pump got the largest rectifier loss but not the greatest conduction loss with higher conduction losses observed for the dishwasher, stove and outlet living-room. These three fuses got loads that often operate at high power which generates a high current according to (2.6), and since conduction losses are proportional to the squared current, according to (2.4), these fuses will have a high conduction loss.

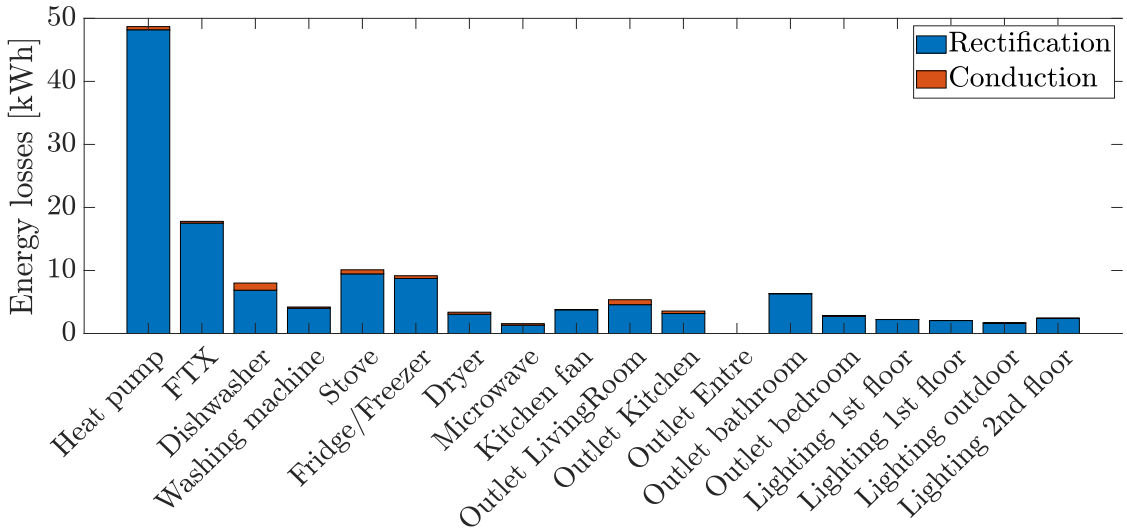

Figure 4.1: Energy losses for each fuse in the villa for the reference case with constant efficiency for PECs.

4.2 Constant vs. Dynamic PEC Efficiencies

Figure 4.2 shows the total annual losses for each case with both dynamic and constant PEC efficiency. In every case, the one with dynamic efficiency for PECs is beaten by the one with constant efficiency for PECs. The difference was the smallest for the 230 VAC case between the constant and dynamic efficiency an increase of 79% was observed. The biggest difference was found for the 380 VDC case where rectification loss went up by 313%. This aligns with results from another study concluding that a constant efficiency underestimates the converter losses [22]. In Fig. 4.2, DC cases are more affected by the transition from constant PEC efficiencies to dynamic PEC efficiencies than the AC case. DC cases are more affected by dynamic PEC efficiencies because the grid-tied rectifier has to work over a much wider range since it rectifies all loads at the same time according to (3.6). In the AC case, all loads have individual rectifiers and a majority of loads are binary. Binary loads are working at 100% of their rated power, when turned on, which leads to a rectifier efficiency of 97.4%, see Fig. 3.7.

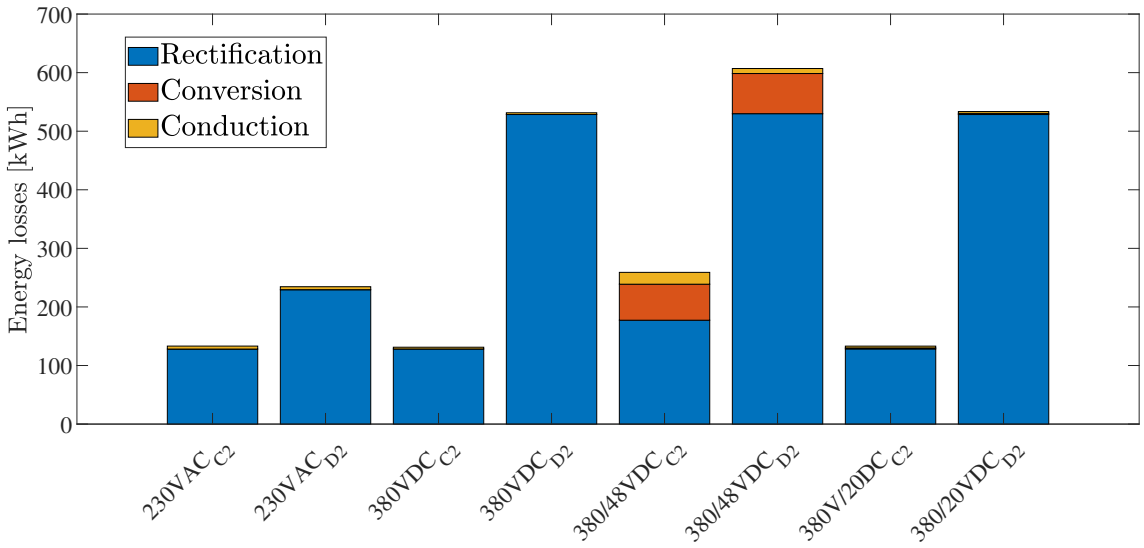

Figure 4.2: Dynamic efficiency is compared to constant efficiency for all optimized cases.

4.3 Optimal vs. Standard Cable Area

The conduction losses for the dynamic cases are presented in Fig. 4.3. For three cases the effect of the optimization was insignificant, for the 380/48 VDC case an improvement can be seen for the conduction losses. Conduction losses are more than halved from 21.4 to 8.6 kWh when the cross-sectional areas are optimized for cables in the 380/48 VDC case. The relatively small effect of the optimization on the 380/20 VDC, case which should have seen the largest improvement can be explained by the power limit for USB-C at 100 W. The largest improvement, should be seen for the 380/20 VDC case since the current increases when the voltage is lowered

according to (2.6) which leads to increasing conduction losses. Due to the power limit for USB-C only two fuses were able to operate on the 20 VDC level network, and few loads with low power leads to small conduction losses. Table 4.1 shows the result for all cases with optimized cable sizes. The last column displays the overall efficiency for each case and is calculated according to (3.7).

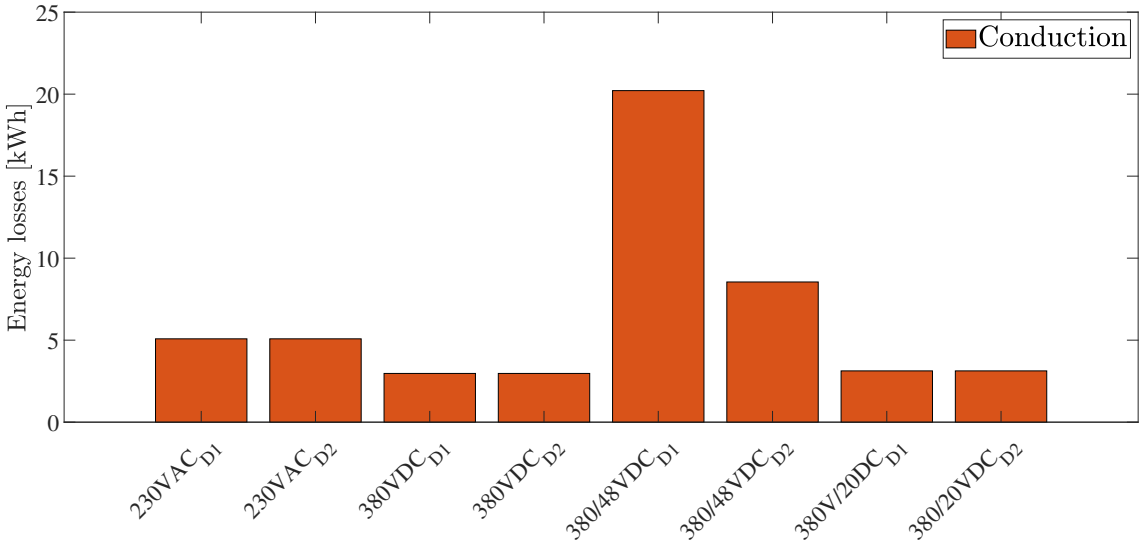

Figure 4.3: All cases are compared with each other to examine the effect of optimizing the cable areas.

Table 4.1: Summary of results for all optimized cases.

Case	Rect	Conv	Line	Total loss	Load	Energy demand	η
230_{C2} [kWh]	128	0	5.1	133	5832	5965	97.8
230_{D2} [kWh]	229	0	5.1	235		6067	96.1
380_{C2} [kWh]	128	0	3	131		5963	97.8
380_{D2} [kWh]	529	0	3	532		6364	91.7
$380/48_{C2}$ [kWh]	129	45	8.6	183		6015	96.9
$380/48_{D2}$ [kWh]	530	69	8.6	607		6439	90.6
$380/20_{C2}$ [kWh]	128	1.7	3.1	133		5965	97.8
$380/20_{D2}$ [kWh]	529	1.9	3.1	534		6367	91.6

4.4 Cases without the Heat Pump

Figure 4.1 showed that the heat pump was by far the greatest energy consumer in the house. Since there are other ways to heat up a building than using a heat pump, the cases were run without the heat pump. In Fig. 4.4 the total load profile with and without the heat pump is plotted as histograms. Each bar in Fig. 4.4 represent how many operating points it is in every 0.5% interval of P_{max} of the bi-directional converter. Figure 4.4 shows how values are shifted to lower loadings when the heat pump is removed, which leads to a lower efficiency for the grid rectifier according to

the efficiency characteristic in Fig. 3.7. The majority of the output from the load profile are below 20% of P_{max} which indicates an oversized P_{max}. In Fig. 4.5, P_{max} is dimensioned by the highest measured operating point of the load profile which evens out the load profile over a wider range of P_{max} and increase the efficiency. Table 4.2 shows results for cases run with dynamic efficiency but without the heat pump.

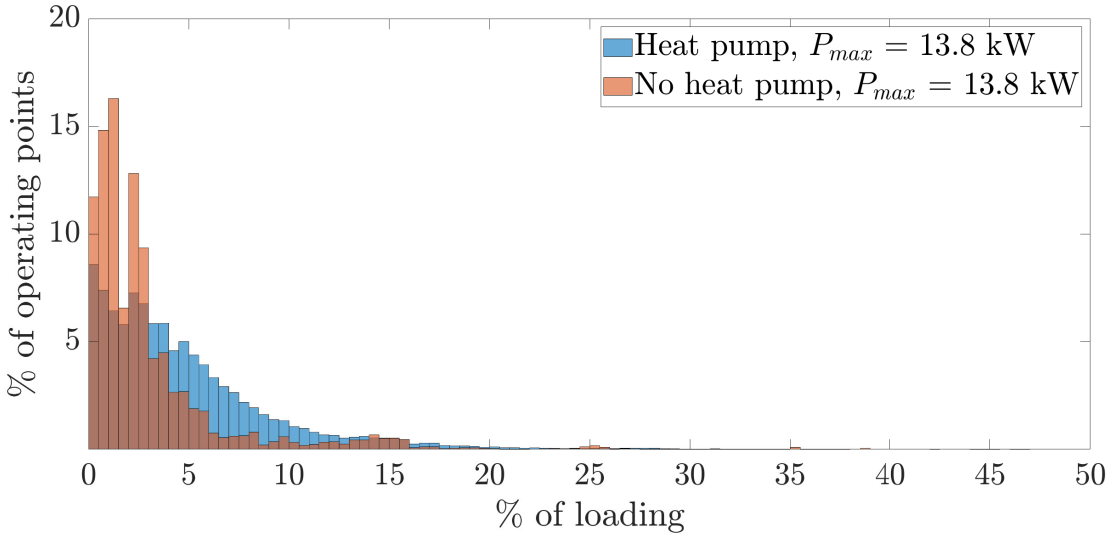

Figure 4.4: The blue bars is the load profile with the heat pump included and the red bars is the load profile with the heat pump excluded. All values from the two load profiles have been sorted into 0.5% intervals depending on their percentage of P_{max}.

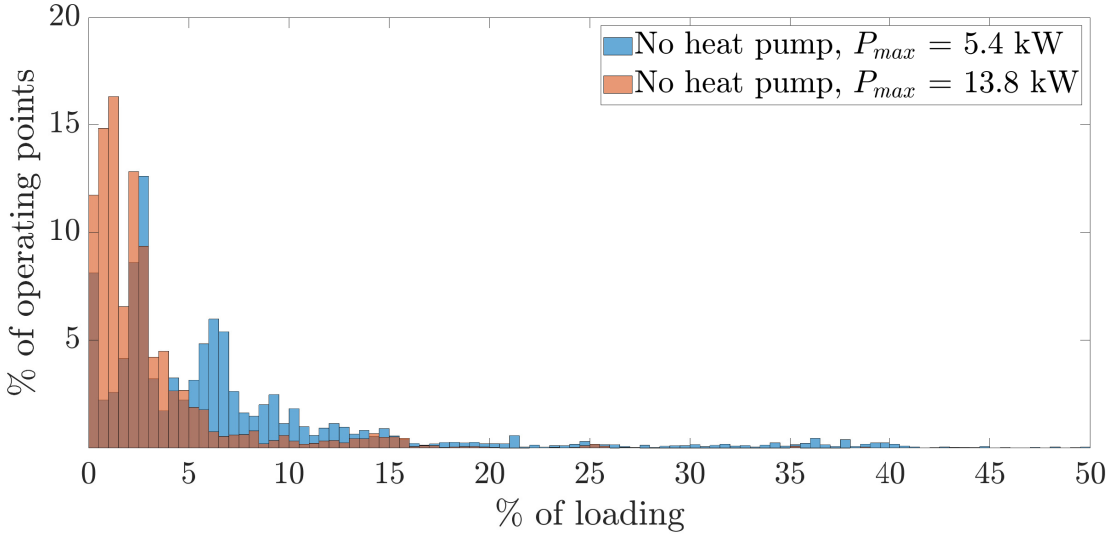

Figure 4.5: Both the blue and red histogram are load profiles without the heat pump. Difference between the histograms is their P_{max} which is set to 5.4 kW for the blue and 13.8 kW for the red histogram. All values from the two load profiles have been sorted into 0.5% intervals depending on their percentage of P_{max}.

Table 4.2: Summary of results for all cases with optimized cable sizes when the heat pump is excluded.

Case	P_{max}	**Rect**	**Conv**	**Line**	**Total loss**	**Load**	**Energy demand**	η
230_{D2} [kWh]	Ind.	102	0	4.6	107		3748	97.2
380_{D2} [kWh]	13.8	557	0	2.5	560		4202	86.7
380_{D2} [kWh]	5.4	227	0	2.5	229		3871	94.1
$380/48_{D2}$[kWh]	13.8	560	69	8.1	636	3641	4278	85.1
$380/48_{D2}$[kWh]	5.4	229	69	8.1	306		3947	92.3
$380/20_{D2}$[kWh]	13.8	558	2	2.7	562		4204	86.6
$380/20_{D2}$ [kWh]	5.4	227	2	2.7	231		3873	94.0

For the 230 VAC case, the losses dropped while for the other cases the losses increased compared to the results with the heat pump included in Table 4.1. Since the 230 VAC case uses individual rectifiers, the efficiency is not so affected by the exclusion of the heat pump. The individual rectifiers will continue working at the load-dependent efficiency for 100% loading for all "ON/OFF" loads. For the DC cases, the rectifier works at such low efficiency that the losses increase even if the heat pump is removed. If the grid-tied rectifier is dimensioned by the highest measured operating point for all the DC cases, load profiles are smoothed out and the annual rectification losses are reduced by 59% in each case.

4.5 Effect of Chosen Power Electronic Rated Power

Figure 4.6 displays the effect of P_{max} on the efficiency curve for the rectifier. The main fuse is assumed to be 20 A which results in a maximum power output of 13.8 kW for the cases. P_{max} is set to 6.36 kW which is the maximum power output from the synthetic load profile seen in Fig. 3.4. Efficiency improves since the converter works at a higher percentage of the maximum load more often when P_{max} is lowered according to (3.6), which generates a higher efficiency. Since P_{max} is more than halved between the dynamic efficiency curves in Fig. 4.6, the loading is twice as high for the case with lower P_{max}. Efficiency is affected by the halved P_{max}, especially when the PECs work below 10% of their maximum capacity. Even when P_{max} is set to 6.36 kW, the result in Fig. 4.6 shows that a dynamic efficiency still does not come close to competing with constant efficiency. The annual rectification loss is reduced by 44.3% when P_{max} is adjusted to 6.36 kWh for the 380 VDC case with load-dependent efficiency, still 130% higher than the annual rectification loss for the 380 VDC case with constant efficiency.

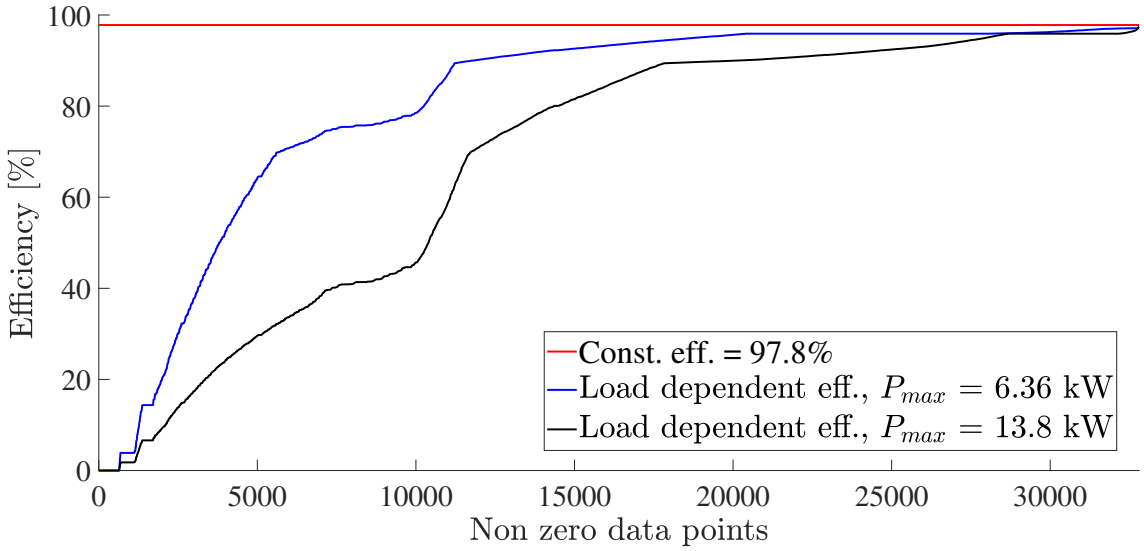

Figure 4.6: Three efficiency curves were one is constant at 97.8% and two are load dependent with different P_{max}.

4.6 Life Cycle Cost

Table 4.3 shows the results for the LCC calculations. In columns 1–3, the material cost, energy cost for 1 year and energy cost for 30 years are listed, respectively. These numbers are used as inputs in (3.8) to compute the results in columns 4 and 5. For each case there are two rows with results, the first row contains the results for the cases run with standard sized cables and the second row contains the cases with optimized sized cables. In many cases there was no economical winning by scaling up cables and the results were the same in both cases for standard and optimized sized cables. In Table 4.3 the second row is therefore filled with "-" to show when no

improvements were made. Only in the 380/48 VDC case changes were made to the cables cross-sectional areas, this is due to the fact that several loads are connected to the 48 VDC. According to (2.6), the current increase as a result of a lower voltage which leads to higher conduction losses according to (2.4). This suggest that cables in the 380/20 VDC case should be optimized. No changes were made for cable cross-sectional areas in the 380/20 VDC case because almost no loads were fed by 20 VDC due to the power limit for the 20 VDC voltage network.

Table 4.3: Summary of material, energy costs and LCC costs for the model of the villa over 1 year and a 30 year period.

Case	Material Cost [SEK]	Energy Cost 1 year [SEK]	Energy Cost 30 year [SEK]	LCC 1 Year [SEK]	LCC 30 Year [SEK]
230_C	2316	254	4094	2569	6410
	-	-	-	-	-
230_D	2316	447	7210	2763	9526
	-	-	-	-	-
380_C	1884	250	4035	2134	5919
	-	-	-	-	-
380_D	1884	1012	16340	2896	18224
	-	-	-	-	-
$380/48_C$	2136	492	7947	2628	10083
	2219	470	7583	2689	9802
$380/48_D$	2136	1101	18155	3261	20291
	2219	657	17769	3320	19988
$380/20_C$	1982	254	4092	2236	6074
	-	-	-	-	-
$380/20_D$	1982	1018	16249	3000	18411
	-	-	-	-	-

5
Discussion

5.1 Social, Ethical and Sustainable Aspects of DC Grids

Since DC grids are still in an early stage of development it will probably not be introduced to the broad market for some time. Two obstacles that DC grids face are lack of standards and low knowledge among workers. From a safety point of view a DC system may be a safer option as it does not lead to involuntary contractions of the muscles which AC can do [28].

Solar power is related when it comes to DC grids and for off grid it could be a setup to use a pure DC grid with solar power and batteries to get energy in remote regions.

5.2 Future Work

There are several interesting ways to continue the work based on the findings in this report, some suggestions are listed below.

- Solar power and batteries are interesting in both off grid and grid-tied setups. Adding solar power and batteries to the existing setup is a next step. Both solar panels and battery are DC driven which makes them an interesting for a DC grid to reduce rectification losses.
- Increase the resolution of the load profiles. Now, a 15-minute average is used, which doesn't sound long but power spikes could easily be hidden. It also effects the conduction losses and propagates into the PECs efficiencies and if dynamic PECs efficiency is used, a small power difference can have an impact on the efficiency as seen in Fig. 4.4.
- A constant energy price was used which does not reflect reality where the energy price fluctuate during an year due to several factors. Therefore fluctuating energy price could be used based on e.g. statistics of energy prices from earlier years to get a characteristic.
- USB-c was not investigated further than from a voltage level point of view. There are further possibilities to explore such as Internet of Things (IoT). Internet of things is the collective name for electronics devices that communicate with each-other, IoT is used in smart-grids. An example of IoT that could be investigated for this project is that appliances could communicate with each-other and run at the same time if it would increase the efficiency of

the grid-tied rectifier in the DC cases.

6
Conclusion

From results found in this report it can be concluded that with a constant efficiency for rectifiers and converters the 380 VDC case attained the best performance with an efficiency at 97.8%. Least efficient was the 380/48 VDC system with an efficiency at 96.9%. With constant efficiency for PECs, there was a non-significant difference between 380 VDC and 230 VAC of 0.01% in favor of 380 VDC. The 380 VDC case had higher rectification losses but lower conduction losses than 230 VAC case and ended up as the most efficient alternative.

In cases with dynamic efficiencies none of the DC cases compete with the AC case. The 230 VAC reference case reached an efficiency of 96.1% whereas the 380/48 VDC had the lowest performance with an efficiency of 90.6%. It should be mentioned that the 48 VDC is introduced to increase the personnel safety of the system and not increase the efficiency.

Cases with dynamic efficiencies performed worse compared to their corresponding cases with constant PECs efficiencies. Although P_{max} were optimized for the dynamic cases, they still could not measure up to the constant efficiency cases.

When cases were tested without the heat pump the efficiency for the 230 VAC case improved while for the DC cases the efficiency decreased due to an increase in rectification losses.

From the LCC it can be concluded that there was no optimizing to be made for the 230 VAC, 380 VDC or 380/20 VDC cases, only in the 380/48 VDC case was an optimizing made. Savings can be considered negligible since only 281 SEK and 303 SEK were saved for the constant respectively dynamic converter efficiencies in the 380/48 VDC case over 30 years.

Bibliography

[1] International Energy Agency. "Key World Energy Statistics 2018". In: (2018), pp. 2, 11. URL: %7Bwww.iea.org/statistics/.%7D.

[2] Stephanie Sammartino McPherson. *War of the Currents: Thomas Edison vs Nikola Tesla*. Twenty-First Century Books, 2012.

[3] Jacobus Daniel Van Wyk and Fred C Lee. "On a future for power electronics". In: *IEEE Journal of Emerging and Selected Topics in Power Electronics* 1.2 (2013), pp. 59–72.

[4] Brock Glasgo, Inês Lima Azevedo, and Chris Hendrickson. "How much electricity can we save by using direct current circuits in homes? Understanding the potential for electricity savings and assessing feasibility of a transition towards DC powered buildings". In: *Applied Energy* 180 (2016), pp. 66–75.

[5] Vagelis Vossos, Karina Garbesi, and Hongxia Shen. "Energy savings from direct-DC in US residential buildings". In: *Energy and Buildings* 68 (2014), pp. 223–231.

[6] Patrik Ollas. "Energy Savings Using a Direct-Current Distribution Network in a PV and Battery Equipped Residential Building". PhD thesis. Chalmers Tekniska Hogskola (Sweden), 2020.

[7] Kiran Siraj and Hassan Abbas Khan. "DC distribution for residential power networks—A framework to analyze the impact of voltage levels on energy efficiency". In: *Energy Reports* 6 (2020), pp. 944–951.

[8] Hasan Erteza Gelani et al. "AC vs. DC distribution efficiency: Are we on the right path?" In: *Energies* 14.13 (2021), p. 4039.

[9] Faizan Dastgeer and Akhtar Kalam. "Efficiency comparison of DC and AC distribution systems for distributed generation". In: *2009 Australasian Universities Power Engineering Conference*. IEEE. 2009, pp. 1–5.

[10] Ander Goikoetxea et al. "DC versus AC in residential buildings: Efficiency comparison". In: *Eurocon 2013*. IEEE. 2013, pp. 1–5.

[11] A Sannino, G Postiglione, and MH Bollen. "J.(2003). Feasibility of a DC network for commercial facilities". In: *IEEE Trans Ind Appl* (), pp. 1499–507.

[12] International Electrotechnical Commission Standard. "Conductors of insulated cables". In: (2004).

[13] *Single Phase Rectification*. URL: https://www.electronics-tutorials.ws/power/single-phase-rectification.html (visited on 08/30/2022).

[14] H Wen and W Xiao. "Bidirectional dual-active-bridge dc-dc converter with triple-phase-shift control". In: *2013 Twenty-Eighth Annual IEEE Applied Power Electronics Conference and Exposition (APEC)*. IEEE. 2013, pp. 1972–1978.

[15] RISE. *Nu flyttar simuleringsfamiljen ut från Forskningsvillan*. URL: https://www.ri.se/sv/press/nu-flyttar-simuleringsfamiljen-ut-fran-forskningsvillan (visited on 08/30/2022).

[16] RISE. *Demo site 1. Borås and Varberg, Sweden*. URL: http://need4b.eu/?page_id=11706&lang=en (visited on 08/30/2022).

[17] Elgiganten. *Vitvaror*. URL: https://www.elgiganten.se/vitvaror (visited on 09/26/2022).

[18] M Padhma. *End-to-End Introduction to Evaluating Regression Models*. URL: https://www.analyticsvidhya.com/blog/2021/10/evaluation-metric-for-regression-models/ (visited on 09/30/2022).

[19] Fatih Issi and Orhan Kaplan. "The determination of load profiles and power consumptions of home appliances". In: *Energies* 11.3 (2018), p. 607.

[20] Manisa Pipattanasomporn et al. "Load profiles of selected major household appliances and their demand response opportunities". In: *IEEE Transactions on Smart Grid* 5.2 (2013), pp. 742–750.

[21] T Thiringer et al. "Besparingspotential för likströmsdistribution-en förstudie". In: *Chalmers University of Technoology, Tech. Rep* (2017).

[22] Patrik Ollas et al. "Increased photovoltaic utilisation from direct current distribution: Quantification of geographical location impact". In: *Progress in Photovoltaics: Research and Applications* 29.7 (2021), pp. 846–856.

[23] Brock Glasgo, Inês Lima Azevedo, and Chris Hendrickson. "Expert assessments on the future of direct current in buildings". In: *Environmental Research Letters* 13.7 (2018), p. 074004.

[24] Rini Nur Hasanah et al. "DC-DC Converter for USB-C Power Adapter in Residential DC Electricity". In: *2019 IEEE Conference on Energy Conversion (CENCON)*. IEEE. 2019, pp. 207–212.

[25] ELFA. *Kopplingstråd*. URL: https://www.elfa.se/sv/kablar-och-ledningar/kopplingstrad/kopplingstrad/c/cat-DNAV_PL_091205?q=*&sort=ProductNumber (visited on 08/30/2022).

[26] Werner Wetekamp. "Net Present Value (NPV) as a tool supporting effective project management". In: *Proceedings of the 6th IEEE International Conference on Intelligent Data Acquisition and Advanced Computing Systems*. Vol. 2. IEEE. 2011, pp. 898–900.

[27] Konsumenternas energimarknadsbyrå. *Konsumentpriser på el i Europa för hushållskunder*. URL: https://www.energimarknadsbyran.se/media/1586/konsumentpriser-pa-el-i-europa-for-hushallskunder.pdf (visited on 09/26/2022).

[28] A. Sannino, G. Postiglione, and M.H.J. Bollen. "Feasibility of a DC network for commercial facilities". In: *Conference Record of the 2002 IEEE Industry Applications Conference. 37th IAS Annual Meeting (Cat. No.02CH37344)*. Vol. 3. 2002, 1710–1717 vol.3. DOI: 10.1109/IAS.2002.1043764.

A

Appendix 1

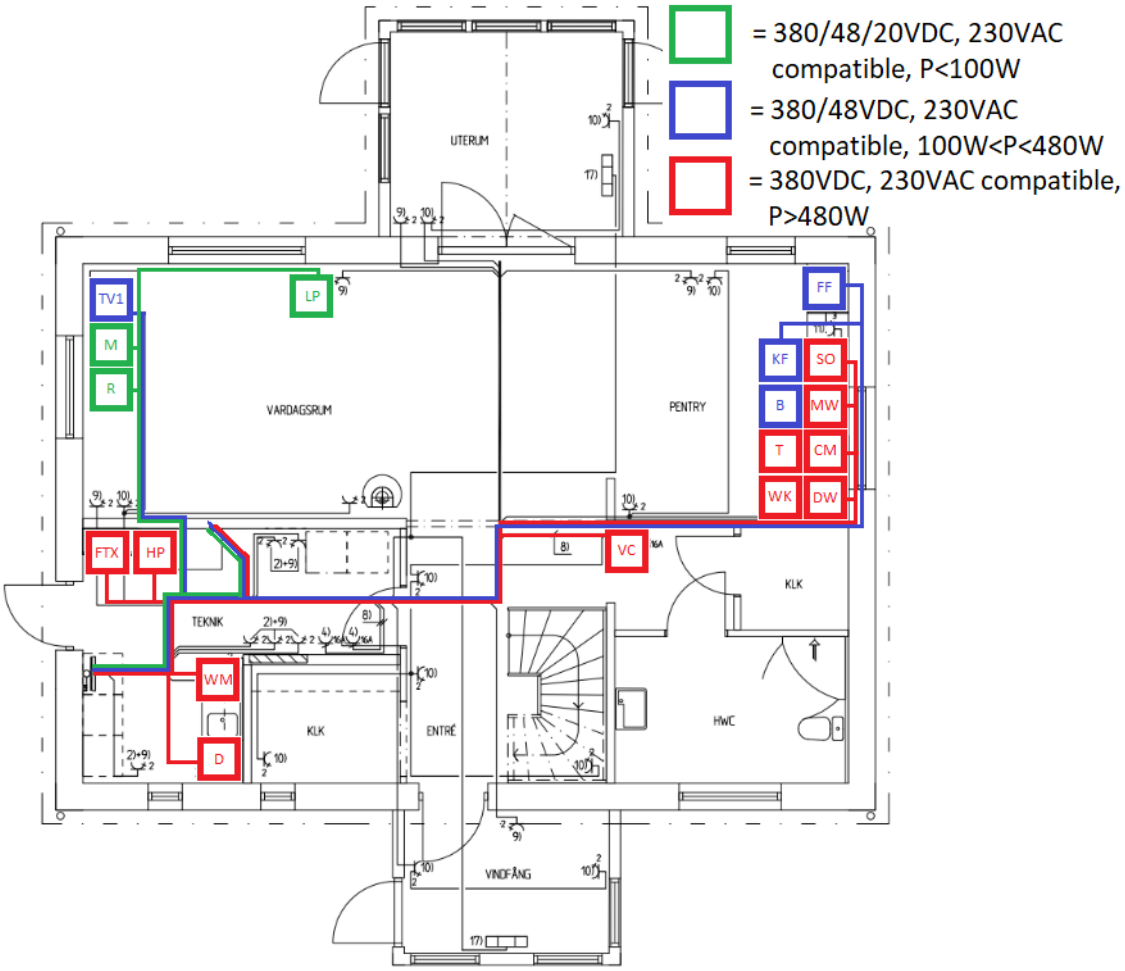

Figure A.1: Layout of stationary and outlet connected appliances for the first floor.

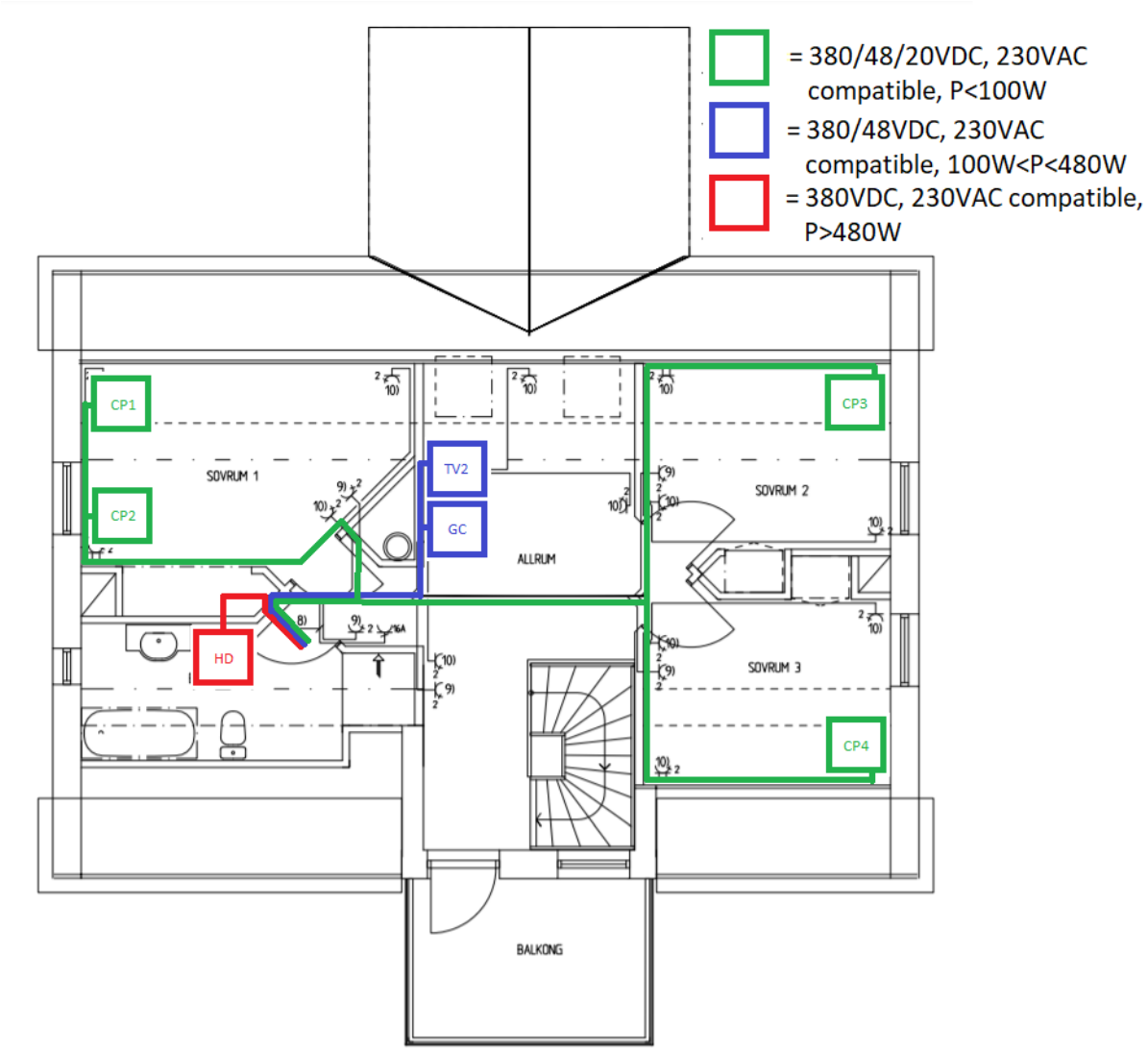

Figure A.2: Layout of stationary and outlet connected appliances for the second floor.

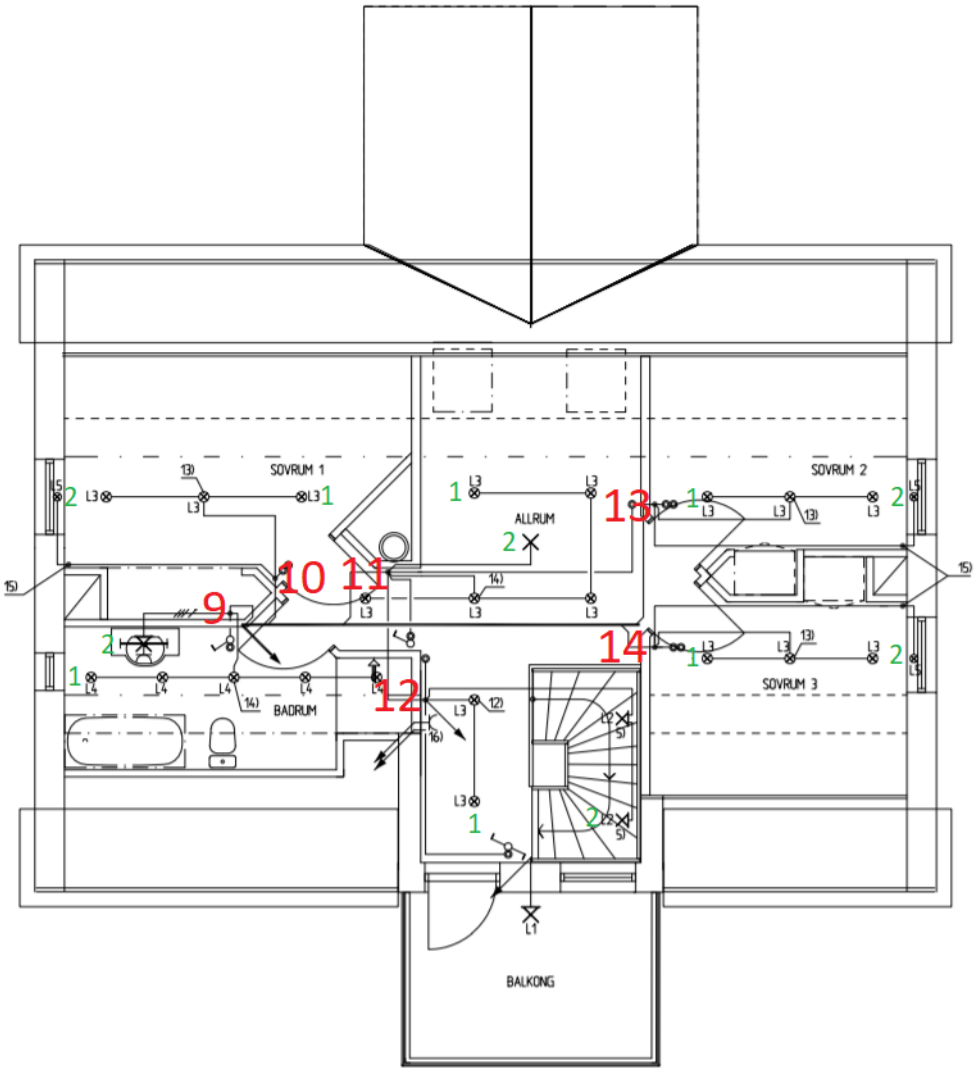

Figure A.3: Layout of stationary and outlet connected appliances for the second floor.

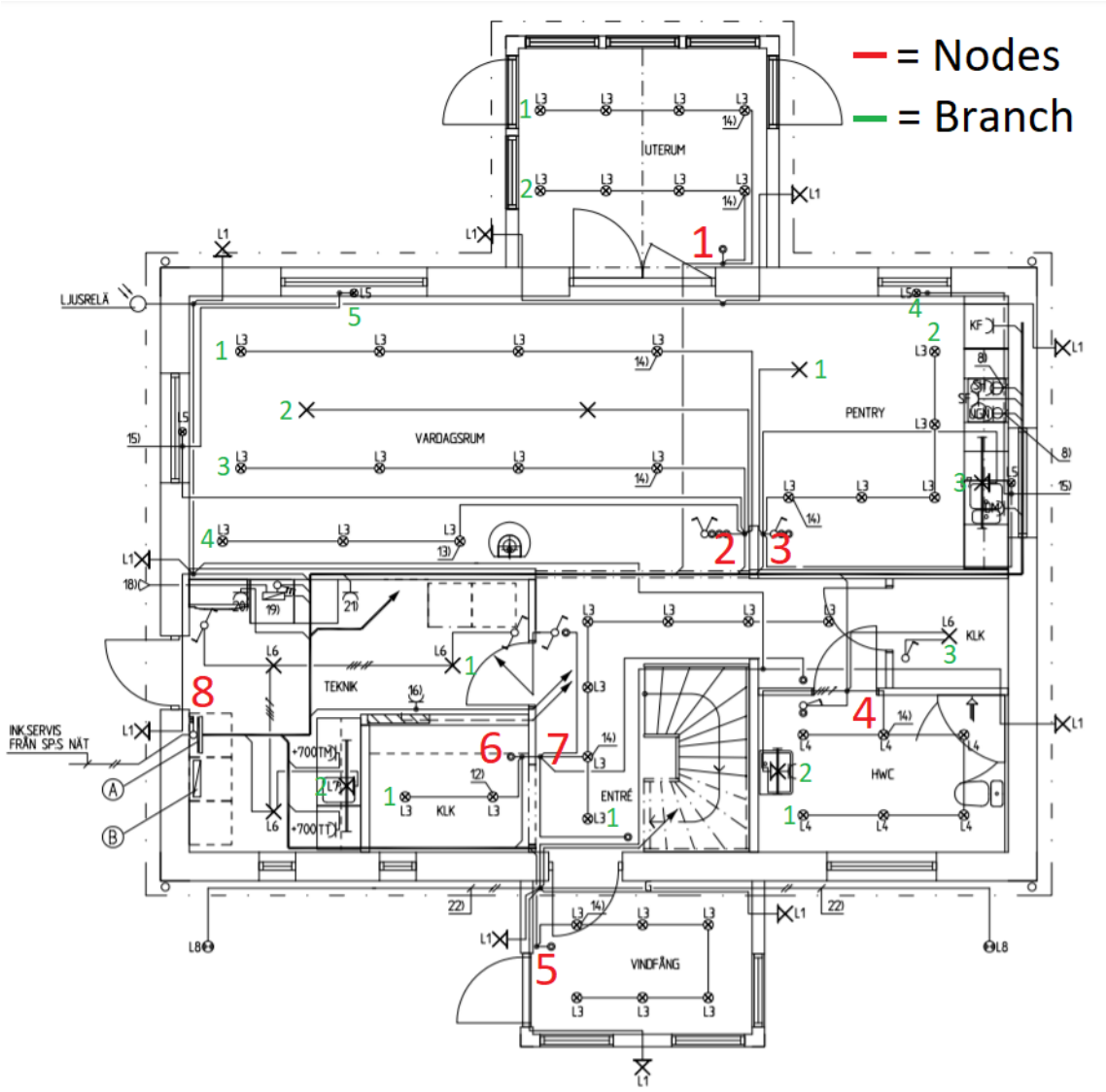

Figure A.4: Layout of stationary and outlet connected appliances for the second floor.

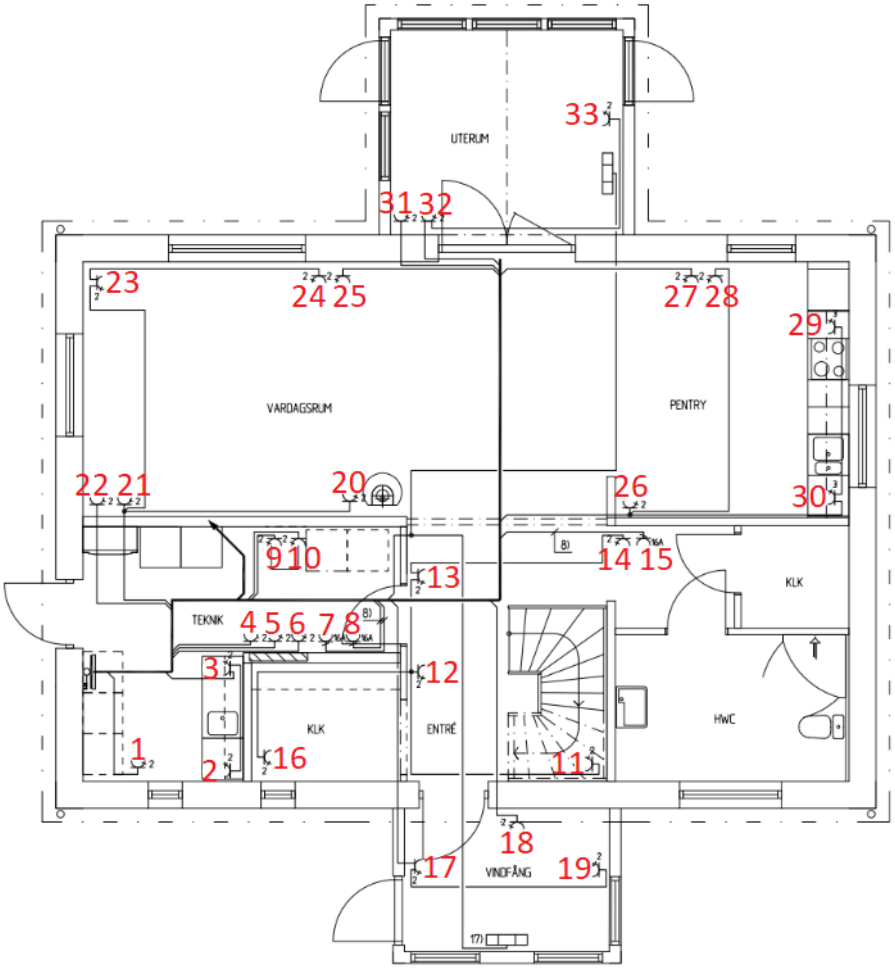

Figure A.5: Layout of stationary and outlet connected appliances for the second floor.

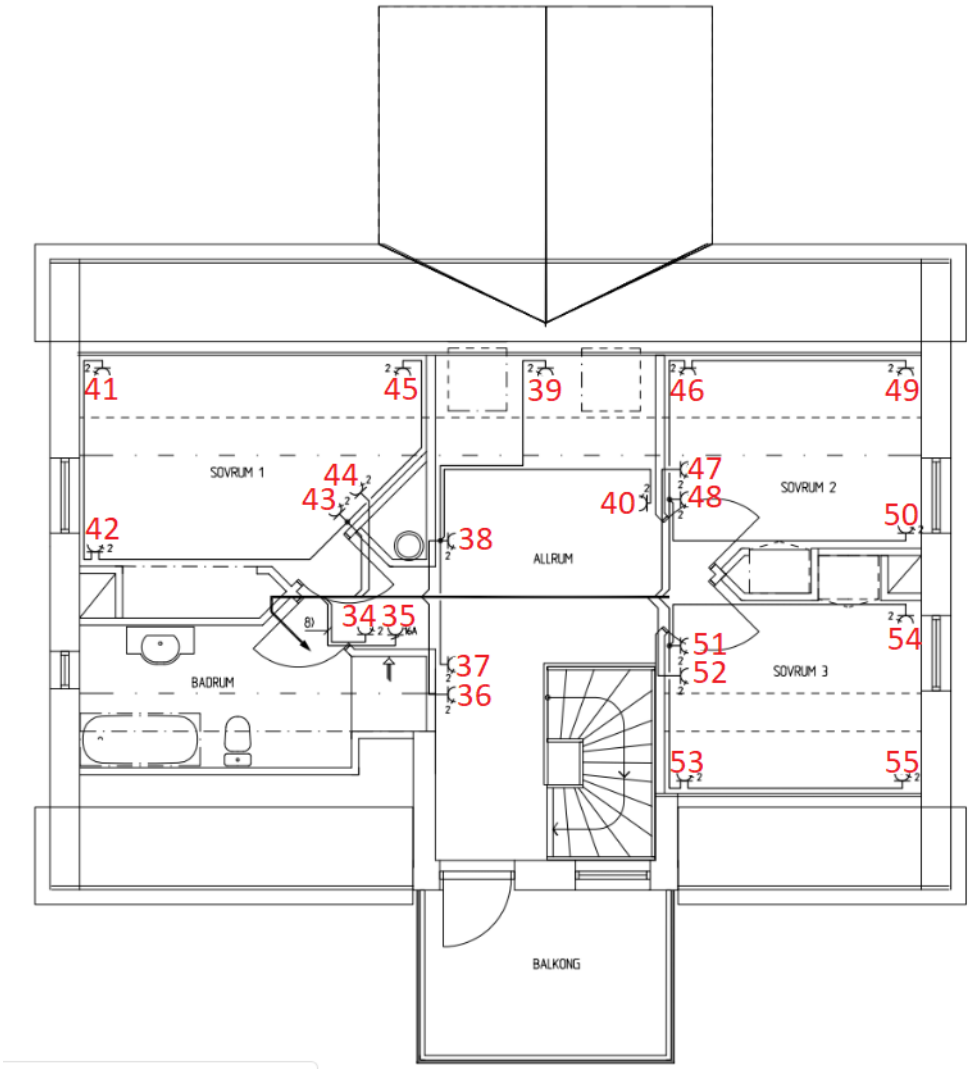

Figure A.6: Layout of stationary and outlet connected appliances for the second floor.

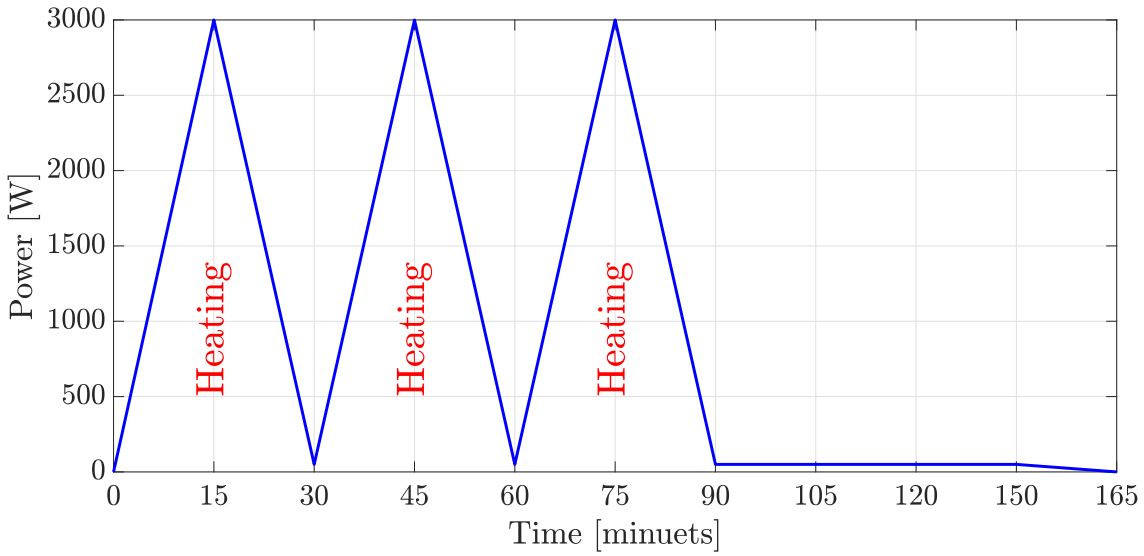

Figure A.7: Load profile for a dryer program.

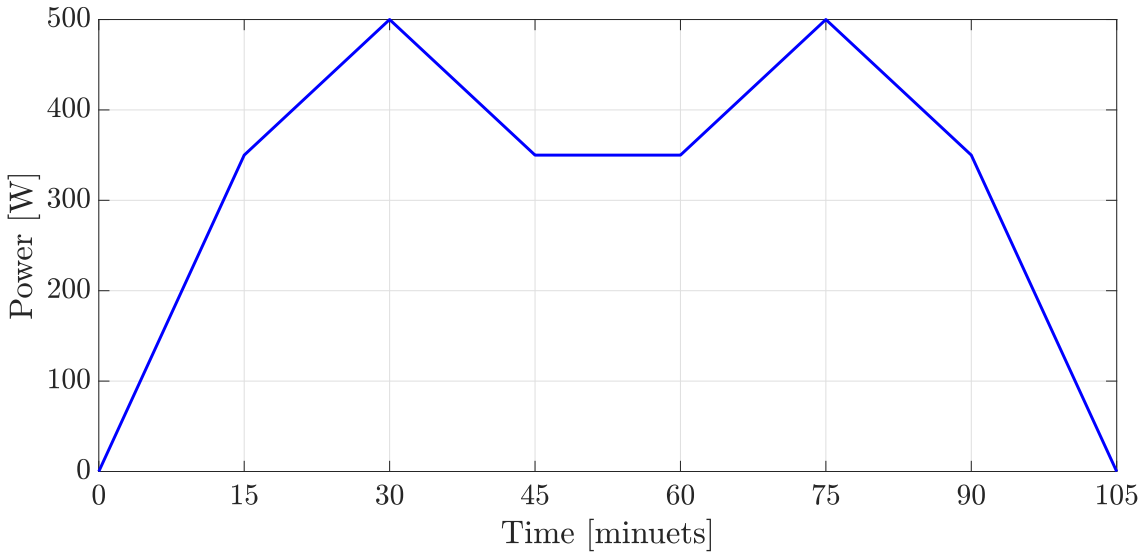

Figure A.8: Load profile for a washing machine program.